CSIRO PUBLISHING

Invertebrate Systematics, 2020, **34**, 837–870
https://doi.org/10.1071/IS20022

The more the merrier: unparalleled sympatric species richness in a sea spider genus (Pycnogonida : Callipallenidae : *Pallenella*) from Tasmanian waters

Georg Brenneis [A,B,F], *Claudia P. Arango* [C], *Prashant P. Sharma* [D] *and Martin Schwentner* [E]

[A]Cytologie und Evolutionsbiologie, Zoologisches Institut und Museum, Universität Greifswald, Soldmannstraße 23, Haus 6.1, D-17489 Greifswald, Germany.
[B]Neuroscience Program, Wellesley College, 106 Central Street, Wellesley, MA 02481, USA.
[C]Biodiversity and Geosciences Program, Queensland Museum, PO Box 3300, South Brisbane, Qld 4101, Australia.
[D]Department of Integrative Biology, University of Wisconsin–Madison, 352 Birge Hall, 430 Lincoln Drive, Madison, WI 53706, USA.
[E]Naturhistorisches Museum Wien, Burgring 7, AT-1010 Vienna, Austria.
[F]Corresponding author. Email: georg.brenneis@gmx.de

Abstract. Southern Australian waters feature remarkably diverse assemblages of the sea spider family Callipallenidae Hilton, 1942. The most speciose of the three Australian-endemic genera currently recognised has been known as *Meridionale* Staples, 2014, but is here reinstated under the name *Pallenella* Schimkewitsch, 1909 based on its type species *Pallenella laevis* (Hoek, 1881). This genus includes several brightly coloured forms that occur in high abundance on arborescent bryozoans. However, considerable similarity of congeners and scarcity of diagnostic characters continue to render species delineation in this genus challenging. Using an integrative taxonomic approach, we combine detailed morphological investigation with analysis of two genetic markers (mitochondrial cytochrome *c* oxidase subunit I, and nuclear rDNA including internal transcribed spacers 1 and 2) to explore the extraordinary species richness of the genus *Pallenella* in south-east Tasmania. In agreement with our morphology-based segregation of different species and morphotypes, we recovered well-supported corresponding clades in the genetic analyses. Strong mito-nuclear concordance in the two markers supports the inference of sustained reproductive isolation between the sympatrically occurring forms. Based on these findings, we distinguish a total of 13 Tasmanian congeners, representing the most diverse assemblage of sympatric species in the same microhabitat reported for a single pycnogonid genus. Within this assemblage, we (1) record the type species *P. laevis* for the first time after almost 150 years, (2) delineate the two Tasmanian morphotypes of the provisional '*variabilis*' complex, and (3) describe two species new to science (*P. karenae*, sp. nov., *P. baroni*, sp. nov.). Despite considerable genetic divergences between most congeners, only few and often subtle characters are found to be suitable for morphology-based delineation. Notably, colouration of living specimens is suggested to be informative in some cases. For morphology-based species identification of preserved specimens, a key relying on combinations of characters rather than single diagnostic features is proposed.

Keywords: biodiversity, cryptic species, cytochrome *c* oxidase subunit I, internal transcribed spacers, integrative taxonomy, *Meridionale*, *Orthoscuticella*, Pantopoda, *Pseudopallene*.

Received 30 March 2020, accepted 28 June 2020, published online 11 November 2020

Introduction

Pycnogonida, or sea spiders, is a group of marine, epibenthic arthropods with a cosmopolitan distribution in the world's oceans (Arnaud and Bamber 1987). The phylogenetic position of sea spiders has been contested (Dunlop and Arango 2005), but presently they are securely placed in the Chelicerata, where they form the sister group to all remaining extant taxa (Legg *et al*. 2013; Ballesteros *et al*. 2019; Lozano-Fernandez *et al*. 2019). Owing to their unique body architecture, sea spiders are readily recognisable, being characterised by a very small body that bears an anterior proboscis and four pairs of long legs (in a few genera even five or six pairs).

Pycnogonids are often well camouflaged in their natural habitats, where they prey on sessile or slow-moving invertebrates. Owing to this and the comparably small size of many shallow-water species, they are among the most

understudied taxa of the benthic fauna. To date, ~1350 species have been formally described (Bamber *et al*. 2020), but new species continue to be discovered in various marine habitats worldwide (e.g. Arango and Linse 2015; Cano-Sánchez and López-González 2019; Lucena *et al*. 2019; Staples 2019). Beyond this, the use of genetic markers in conjunction with morphological reinvestigation has revealed previously unrecognised species diversity and continues to clarify taxonomy and biogeography of morphologically variable species complexes, especially in sub-Antarctic and Antarctic waters (Arango *et al*. 2011; Dietz *et al*. 2015*a*, 2015*b*; Dömel *et al*. 2015, 2017, 2019, 2020; Soler-Membrives *et al*. 2017; Collins *et al*. 2018). Outside of the Southern Ocean region, however, such integrative taxonomic approaches are still rare in Pycnogonida (Stevenson 2003; Arango and Brenneis 2013; Sabroux *et al*. 2019).

The cosmopolitan sea spider family Callipallenidae Hilton, 1942 currently includes 18 genera and ~150 species (Bamber *et al*. 2020; Staples 2020). All of them are characterised by functional cheliphores, comprising (1) a one-articled scape and (2) the two-articled chela that is being formed by the palm with its protruding immovable finger and the moveable finger. The palps on the other hand are only weakly developed, if present at all. In most genera, female palps are lacking completely, but some exceptions exist, e.g. in *Pseudopallene* Wilson, 1878 and *Bradypallene* Kim & Hong, 1987 with vestigial 'one-articled' palp buds and three-articled palps respectively (Kim and Hong 1987; Staples 2014*a*). In males, palp presence and structure ranges from complete lack to, at most, four articles (Bamber 2010; Staples 2014*a*). In contrast to the palps, oviger structure is significantly more conserved. In most genera, they are 10-articled in both sexes, but exceptional six-articled ovigers occur, e.g. in males of *Cheilopallene* Stock, 1955 (Staples 2015). Further, all callipallenid genera for which developmental data are available share a (partly) embryonised development with an advanced postlarval hatching stage instead of the widespread pycnogonid protonymphon larva (for recent overview see Brenneis *et al*. 2017). Beyond this, however, commonalities between genera are scarce and a review of the family is underway (Staples 2014*a*, 2014*b*, 2015, 2020), which has become even more relevant given strong indications for non-monophyly of Callipallenidae (Ballesteros *et al*. 2020).

Australian waters harbour exceptionally diverse callipallenid assemblages, which encompass the three endemic genera *Bamberene* Staples, 2014, *Stylopallene* Clark, 1963 and *Pallenella* Schimkewitsch, 1909. The latter two genera include several species with unusually conspicuous colouration patterns (e.g. Arango and Brenneis 2013; Staples 1997, 2014*a*, 2014*b*) and in particular in *Pallenella*, this colouration may contrast with the arborescent bryozoans to which they cling and on which they prey. Notably, all members of the genus *Pallenella* had only been recently separated from the genus *Pseudopallene* Wilson, 1878 under the new genus name *Meridionale*, with *M. laevis* (Hoek, 1881) as type species (Staples 2014*a*). However, owing to the introduction of the genus *Pallenella* for the same type species more than a century ago (Schimkewitsch 1909), this genus name has been reinstated here (see Discussion). The known distribution of *Pallenella* ranges from north-western Australia along the entire western and southern coastline and Tasmania up to Queensland in the north-east (Staples 2014*a*). To date, the genus encompasses 15 recognised species (Bamber *et al*. 2020), but species delimitation is quite challenging, as there are only a few diagnostic morphological characters to rely on (Staples 2005, 2007, 2008) and the extent of intraspecific variation is largely unexplored.

In south-east Tasmania, *Pallenella* is very abundant and relatively easy to access by SCUBA diving, which has been taken advantage of in recent studies of pycnogonid development and neuroanatomy (Brenneis and Scholtz 2014; Brenneis *et al*. 2011*a*, 2011*b*, 2013, 2018). Unfortunately, these works were still faced with uncertain and incomplete documentation of the identity of local species (see Stevenson 2003). This was partially resolved by a taxonomic study that pioneered the use of a nuclear rDNA fragment (including internal transcribed spacer regions 1 and 2) in combination with mitochondrial cytochrome *c* oxidase subunit I (*COI*) for species delineation in pycnogonids (Arango and Brenneis 2013). As a result, no less than seven sympatric congeners could be reliably distinguished in the area. However, the status of two additional, very similar morphotypes remained equivocal, and they were provisionally placed in an unresolved '*variabilis*' complex with genetically close congeners from Victoria and New South Wales. Notably, the two '*variabilis*' complex morphotypes from Tasmania can be easily segregated when live, due to distinctive colouration patterns (Arango and Brenneis 2013). One of them is plain yellow, with proboscis and chela fingers typically covered by a dark crust ('black tips': Fig. 1*A–C*) and the other features red longitudinal lines along body and appendage articles ('stripes': Fig. 1*D–F*) similar to marks reported for *Pallenella chevron* (Staples, 2007) from South Australia.

The current study builds on the previous results. Using newly collected material, we combine detailed morphological investigation and analysis of the two genetic markers to further disentangle the extraordinary diversity of Tasmanian *Pallenella*. Based on this approach, we distinguish a total of 13 congeners in the study area. This is the first well documented case of such high sympatric species richness in a single sea spider genus, with members concentrated in a very small area in exceedingly similar microhabitats. The diverse assemblage includes two species new to science and the first record of the genus' type species after 140 years.

Material and methods

Study area and specimen collection

A subset of the specimens studied was previously analysed in Arango and Brenneis (2013). Except for *Pallenella harrisi* (Arango & Brenneis, 2013) from New South Wales, this material had been collected between 2007 and 2009 in shallow waters along a 15-km stretch of coastline near Eaglehawk Neck, south-east Tasmania, between Deep Glen Bay (42°58′18″S, 147°59′22″E) and Waterfall Bay (43°03′35″S, 147°56′55″E). Single individuals were collected further south in Fortescue Bay (43°08′15″S, 147°58′05″E). In October and November 2015, additional animals were collected from the same area by SCUBA

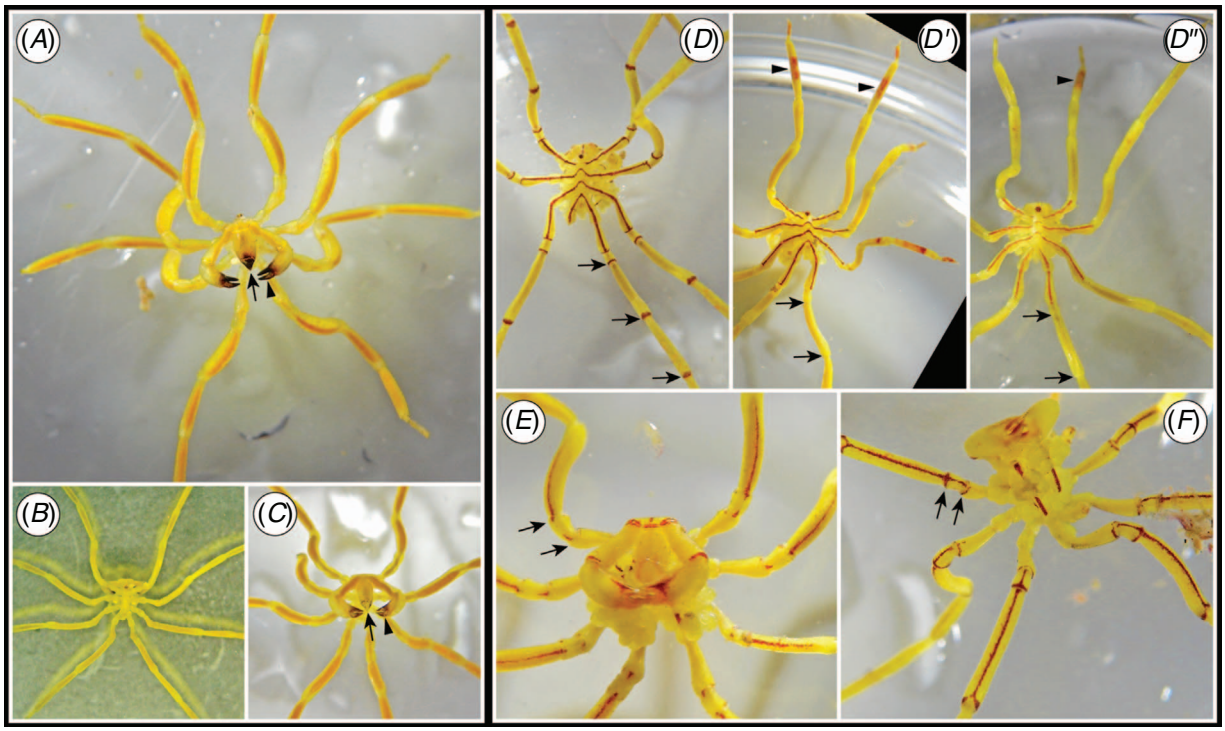

Fig. 1. Live specimens of Tasmanian *P. baroni*, sp. nov. ('black tips') and *P.* cf. *chevron* ('stripes'). (*A–C*) *P. baroni*, sp. nov. Arrows and arrowheads highlight dark crust on proboscis and chela fingers respectively. (*A*) Anteroventral view of female (EN25). (*B*) Dorsal view of male (EN05). (*C*) Ventral aspect of male. Note limited extension and low intensity of dark crust. (*D–F*) *P.* cf. *chevron*, ovigerous males. Arrows highlight distal margins of leg articles with or without red rings. Arrowheads mark broad red bands on tibia 2. (*D*) Dorsal view of specimen 11b. *D′*, Dorsal view of specimen EN18. *D″*, Dorsal view of male with low intensity of stripes. (*E*) Ventral aspect of specimen EN18. (*F*) Ventral aspect of specimen EN19.

diving in 5- to 25-m depth. Specimens were picked by hand from arborescent bryozoans, predominantly of the genus *Orthoscuticella* (Cheilostomata, Catenicellidae) on which pycnogonids prey (Fig. 2*A*). Live animals were photographed before fixation and either directly transferred into absolute ethanol for genetic analyses or preserved in 4% PFA/SW (16% formaldehyde [methanol-free, Electron Microscopy Sciences, CAS # 30525-89-4] diluted 1 : 4 in filtered natural sea water) for morphological investigation. For morphological comparison, a major part of the material from Arango and Brenneis (2013) as well as additional specimens from the 2007–09 collection trips were studied (see Systematics section for individual specimens sorted by species). Further, the male holotype of *Pallenella ambigua* (Stock, 1956) (Zoologisches Museum Hamburg, K17680) was re-examined and photographs of the holotype of *Pallenella chevron* (Staples, 2007) (South Australian Museum, E3681) were consulted. New holotypes have been deposited at the Tasmanian Museum and Art Gallery (TMAG J6267–J6269); all other new specimens studied are housed at the Queensland Museum (QM S111240–111258).

Terminology

Based on its anatomy, the cheliphore (=homologue of the chelicera in other chelicerate taxa) is described as three-articled (scape, palm with immoveable finger, moveable finger). The penultimate and ultimate articles form the chela, which represents one functional unit. To capture the three dimensions of the chela in the morphometric analyses, we distinguish chela length and height, as well as palm depth (Fig. S1*B* of the Supplementary material).

In the present study, the term 'anal tubercle' is given preference over 'abdomen' (widely used in taxonomic literature). This neutral descriptive designation was chosen in order to differentiate the anus-bearing protrusion of pycnogonids from the posterior tagma of hexapods and some crustacean taxa (e.g. Sars 1891 or Brusca and Brusca 2003 for similar use of neutral terminology). Further, it avoids direct homologisation with the opisthosoma of other chelicerate taxa, which would be only partially correct as complete correspondence of the two body regions is challenged by the presence of at least one additional limb-bearing trunk segment in sea spiders (see Dunlop and Lamsdell 2017 for tagmosis in Chelicerata).

Species identification and documentation of external morphology

Identification of species was based on the original descriptions and subsequent taxonomic revisions and keys (Hoek 1881; Haswell 1884; Flynn 1919; Stock 1956, 1973; Staples 1997, 2005, 2007, 2008, 2014*a*; Arango 2009; Arango and Brenneis 2013).

Brightfield and epifluorescence images were taken with a Nikon SMZ25 stereomicroscope, equipped with a Nikon DS-Ri2 camera. Z-stacks were generated with the complementary NIS Elements AR software (ver. 4.51, Nikon Corporation, Tokyo, Japan) and (1) either directly combined into an image with extended depth of field, or (2) exported as tiff-files and subsequently merged using Helicon Focus software (ver. 6.7.1, Helicon Soft, Kharkiv, Ukraine).

A Leica DMI 6000 CS fluorescence microscope equipped with Leica TCS SP5 II scan unit was used to document the oviger compound spines and terminal claw in high resolution. For this purpose, cuticular autofluorescence was elicited with UV and argon laser lines (405- and 488-nm wavelength respectively). Virtual 3D stacks of both signals were edited with the 3-D reconstruction software Imaris (ver. 7.0.0, Bitplane AG, Zurich, Switzerland). Combination of both channels resulted in the best depiction of the structures of interest. All images were processed in Adobe Photoshop (ver. 12.1, Adobe Systems Incorporated, San Jose, CA, USA), applied changes including transformation into greyscale images, cropping, and adjustment of global brightness and contrast. Figures were assembled in Adobe Illustrator (ver. 15.1, Adobe Systems Incorporated).

Measurements and counts

Measurements were performed on images of fixed specimens using the measurement function in NIS Elements AR. Body length was measured dorsally from the anterior margin of the cephalon to the posterior margin of the lateral process of leg 4 (Fig. S1*A*). Body width was measured dorsally across trunk segment 2. Articles of leg 3 were measured from the proximal to the distal joints, with the exception of the tarsus, which was measured along its ventral side. If both legs 3 were missing or in a regenerative state (i.e. distinctly smaller than the other legs), leg 2 was used instead. Addition of leg article measurements resulted in total leg length. We refrained from calculating the leg span for specimens, as an unambiguous definition for this value is lacking (Bamber 2010). Palm depth was measured on dissected chelae positioned so that the articulation plane of the moveable finger pointed upward (i.e. posterior view: Fig. S1*B*). Counts of propodus heel spines and oviger compound spines were performed using epifluorescence stereomicroscopy. The denticulation along the margins of the oviger claw was studied in cLSM scans. For calculation of the average number of propodus heel spines (only for '*variabilis*' morphotypes) only the unpaired major spines were considered (i.e. exclusion of distalmost pair of smaller heel spines). Propodi of legs that were obviously regenerating were excluded, as they almost always bear distinctly fewer spines.

Morphometric analysis of Tasmanian 'variabilis' *morphotypes*

To account for size differences between specimens, measurements are expressed in proportion to overall size. As proxy for the latter, the two variables 'body length' and 'leg length' were considered. Correlation of both variables was tested using the open-source statistical analysis platform R (ver. 3.6.2, see https://www.r-project.org/). Shapiro–Wilk tests were performed to exclude significant deviations from normality in the sample distributions. In both morphotypes, subsequent Pearson correlation testing recovered a strong positive correlation that is well explained by a linear relationship ('black tips': $r = 0.91$, $P < 0.00001$; 'stripes': $r = 0.98$, $P < 0.00001$) (Fig. S1*C*), indicating that both variables are equally suited for the purpose. In concordance with previous studies on pycnogonids (Dietz *et al*. 2015*b*; Dömel *et al*. 2019), we calculated relative values as a proportion of 'body length' (Table S1 of the Supplementary material).

Principal component analysis of relative values was performed with the prcomp() function of the default stats package in R. Analyses were run separately for subadult and adult specimens, once with the full set of measurements and another time with a reduced set (20 *v*. 11 variables respectively). In the latter, several measurements were excluded that were either (1) known to show sex-specific differences (e.g. length of coxa 2), (2) suspected to be less reliable because of its very small size (e.g. tarsus length), (3) found to be inconsistently preserved (e.g. proboscis length varies with pro-/retraction of arthrodial membrane), or (4) showed very strong correlation ($r > 0.9$) with other variables (e.g. palm and moveable finger lengths are both strongly correlated with overall chela length).

DNA sequences

For species identification based on molecular data, DNA fragments targeted were the widely used mitochondrial cytochrome *c* oxidase subunit I (*COI*), or 'barcoding' gene (Hebert *et al*. 2003), and a nuclear rDNA stretch containing *18S* rRNA (partial), internal transcribed spacer 1 (*ITS1*), *58S* rRNA, internal transcribed spacer 2 (*ITS2*) and *28S* rRNA (partial). This nuclear locus is hereafter referred to as '*ITS*'.

Sequences were generated for selected specimens collected in 2015 (Table 1). DNA was extracted from one leg using a DNeasy Blood & Tissue Kit (Qiagen, #69504) according to the manufacturer's protocol (elution in 100–150 µL of elution buffer or ddH_2O). Prior to extraction, midgut and gonad diverticula spanning through the leg were manually removed to avoid potential contamination by gut contents.

Both DNA fragments were amplified by polymerase chain reaction (PCR) using Phusion High-Fidelity DNA polymerase and the 5× HF PCR buffer provided by the manufacturer (ThermoFisher Scientific; #F530L). *COI* was amplified using the LCO1490 and HCO2198 primer pair (Folmer *et al*. 1994) (Table 2) under the following conditions: 3 min of denaturation at 98°C; 38 cycles of 98°C for 30 s, 48°C for 30 s and 72°C for 30 s; final extension at 72°C for 5 min. For *ITS* amplification the ITSRA2 and ITS2.2 primer pair was used (Wörheide 1998) (Table 2) with the following PCR settings: 3 min denaturation at 98°C; 38 cycles of 98°C for 30 s, 55°C for 30 s and 72°C for 50 s; final extension at 72°C for 5 min. PCR products were checked by gel electrophoresis and either cleaned directly (Monarch PCR & DNA Cleanup Kit; New England Biolabs, #T1030S) or by gel purification of the target band (Monarch DNA Gel Extraction Kit, New England Biolabs, #T1020S). Bidirectional Sanger sequencing of purified products was performed at Genewiz (South Plainfield, NJ, USA). *COI* and *ITS* raw sequences were

Table 1. List of specimens used in the genetic analyses, including specimen labels, collection year, museum voucher numbers, as well as GenBank accession numbers for each DNA fragment

Specimens for which sequences were newly generated or previously unpublished are highlighted in bold. Missing data are indicated by an '×'. QM, Queensland Museum; TMAG, Tasmanian Museum and Art Gallery; AM, Australian Museum

Species (field label)	Specimen label	Locality	Collection year	Voucher number	*COI* GenBank number	*ITS* GenBank number
Pallenella						
cf. *ambigua*	**EN07**	**Tasmania**	**2015**	×	×	**MT302591**
	EN10	**Tasmania**	**2015**	**QM S111247**	**MT303088**	**MT302592**
	EN11	**Tasmania**	**2015**	**QM S111247**	**MT303089**	**MT302593**
	EN27	**Tasmania**	**2015**	**QM S111248**	**MT303090**	**MT302594**
baroni, sp. nov. (black tips)	**PSE3**	**Tasmania**	**2009**	**QM S92303**	**MT303106**	**MT302612**
	PSE3b	Tasmania	2009	QM S92303	×	JX196731
	PSE3c	Tasmania	2009	QM S111258	JX196717	×
	EN05	**Tasmania**	**2015**	**TMAG J6268**	**MT303091**	**MT302595**
	EN25	**Tasmania**	**2015**	**TMAG J6269**	**MT303092**	**MT302596**
brevicephala	PSE7	Tasmania	2009	QM S92219	HQ970318	JX196744
	PSE7a	Tasmania	2009	QM S92219	JX196720	JX196742
	PSE7b	Tasmania	2009	QM S92219	JX196719	JX196741
	PSE12	Tasmania	2009	QM S92219	JX196725	JX196746
	TAS28	Tasmania	2007	QM S92219	HM432444	×
cf. *chevron* (stripes)	**EN03**	**Tasmania**	**2015**	**QM S111245**	**MT303093**	**MT302597**
	EN18	**Tasmania**	**2015**	**QM S111244**	**MT303094**	**MT302598**
	EN19	**Tasmania**	**2015**	**QM S111245**	**MT303095**	**MT302599**
	TAS17	Tasmania	2007	QM J92224	JX484741	×
	TAS30a	Tasmania	2007	QM J92224	HM432447	×
constricta	PSE2	Tasmania	2009	TMAG J4519	HQ970314	×
	PSE2a	Tasmania	2009	QM S92223	JX196715	JX196739
	PSE2b	Tasmania	2009	QM S92223	JX196723	JX196740
flava	PSE1	Tasmania	2009	TMAG J4520	HQ970313	×
	PSE1a	Tasmania	2009	QM S92301	JX196714	JX196733
	PSE1b	Tasmania	2009	QM S92301	JX196716	JX196732
	GBTAS	Tasmania	2008	QM S92302	HM381682	×
	EN14	**Tasmania**	**2015**	×	**MT303096**	**MT302600**
karenae, sp. nov. (conc. bands)	**EN15**	**Tasmania**	**2015**	**TMAG J6267**	**MT303097**	**MT302601**
gracilis	PSE6	Tasmania	2009	TMAG J4518	HQ970317	JX196751
	TAS30	**Tasmania**	**2007**	**QM S111251**	×	**MT302602**
harrisi	SHE010	NSW	2009	AM P.90044	HM381709	JX196755
inflata	**TAS 35**	**Tasmania**	**2007**	**QM S111241**	**MT303098**	×
laevis (pale green)	**EN31**	**Tasmania**	**2015**	**QM S111240**	**MT303099**	**MT302603**
	17a	**Tasmania**	**2015**	**QM S111240**	**MT303100**	**MT302604**
	17b	**Tasmania**	**2015**	**QM S111240**	**MT303101**	**MT302605**
pachycheira	TAS21	Tasmania	2007	QM S92222	×	JX196753
	PSE8	Tasmania	2009	QM S92220	×	JX196752
	PSE11a	Tasmania	2009	QM S92220	×	JX196754
	EN01	**Tasmania**	**2015**	×	×	**MT302606**
	EN21	**Tasmania**	**2015**	**QM S111253**	**MT303102**	**MT302607**
	EN35	**Tasmania**	**2015**	**QM S111254**	**MT303103**	**MT302608**
reflexa	PSE5a	Tasmania	2009	QM S92218	×	JX196736
	PSE5b	Tasmania	2009	QM S92218	×	JX196737
	PSE11	Tasmania	2009	QM S92218	×	JX196734
	EN29	**Tasmania**	**2015**	**QM S111255**	**MT303104**	**MT302609**
	EN33	**Tasmania**	**2015**	**QM S111256**	×	**MT302610**
tasmania	PSE4	Tasmania	2009	QM S92216	HM970316	JX196748
	PSE4a	Tasmania	2009	TMAG J4517	JX196718	JX196749
	PSE4b	Tasmania	2009	QM S92216	×	JX196750
	TAS21a	Tasmania	2007	QM S92217	HM432446	×
	TAS35a	Tasmania	2007	QM S92217	HM432456	×
	EN28	**Tasmania**	**2015**	**QM S111252**	**MT303105**	**MT302611**
Austropallene cornigera	POL56	Antarctica		ZSMA20080571	DQ390077.1	JX196727
Nymphon australe	CEA133	Antarctica		in queue for QM registration	GU566140.1	JX196726

Table 2. Primer pairs used for the amplification of the two target DNA fragments

DNA fragment	Primer	Primer sequence	Source
COI	LCO1490	5′-GGT CAA CAA ATC ATA AAG ATA TTG G-3′	Folmer *et al*. (1994)
	HCO2198	5′-TAA ACT TCA GGG TGA CCA AAA AAT CA-3′	
COI	COI_for2	5′-ATY TTT GGD TTN KGA KCH GC-3′	Present study
	COI_rev2	5′-TGT TGR TAH ARR ATW GGR TCH CC-3′	
ITS	ITSRA2	5′-GTC CCT GCC CTT TGT ACA CA-3′	Wörheide (1998)
	ITS2.2	5′-CCT GGT TAG TTT CTT TTC CTC CG-3′	

checked and edited in Geneious R10 (ver. 10.2.6, Biomatters, Ltd, Auckland, New Zealand). *COI* nucleotide sequences were translated to protein sequences (invertebrate mitochondrial code, translation table 5) to confirm absence of stop codons. Sequences were additionally checked by BLASTn search against GenBank to identify and exclude contaminations.

If only contaminated or poor-quality *COI* sequences were obtained with the standard PCR or by gradient PCR (48–52°C annealing temperatures), low-quality amplicons were cloned with a Zero Blunt TOPO PCR Cloning Kit with chemically competent TOP10 OneShot cells (ThermoFisher Scientific, Invitrogen, #K2875-20). After inoculation on LB/ampicillin agar plates at 37°C, up to 10 clones were picked and amplified using the M13 primers which flank the inserts on the vector (53°C annealing temperature). If neither cloning nor repetition of DNA extraction resulted in clean sequences, nested primers (COI_for2, COI_rev2; based on alignment of all *COI* sequences available at this point: Table 2) were used (49°C annealing temperature).

The *ITS* sequence of a single specimen (EN07) was generated in the context of a separate study (Ballesteros *et al*. 2020).

Sequencing raw reads and chromatograms of *COI* and *ITS* generated for our previous study (Arango and Brenneis 2013) were reassessed using Geneious R10 and consensus sequences refined and republished in GenBank (7 × *COI*, 10 × *ITS*).

All new sequences have been deposited in GenBank. Accession numbers as well as specimen labels and voucher numbers at the Tasmanian Museum and Art Gallery and Queensland Museum are listed in Table 1.

Molecular analyses

Both gene fragments were individually aligned using MAFFT (ver. 7.402, see https://mafft.cbrc.jp/alignment/software/; Katoh and Standley 2013) under the L-INS-I criterion. Alignments were conducted twice, once with all available sequences and once including only those specimens for which both gene fragments are available. The full *ITS* alignment features large, poorly aligned regions with extensive indels owing to the two markedly variable *ITS1* and *ITS2* regions. Ambiguously aligned regions were masked with Zorro (Wu *et al*. 2012) and removed using a custom python script (Supplementary file 1) with threshold values of ‘2’ or ‘5’ respectively. Lower thresholds are less strict and remove fewer nucleotides.

To delimit putative species, we employed a combination of phylogenetic analyses and genetic distance analyses (i.e. automated barcoding gap discovery (ABGD): Puillandre *et al*. 2012). Phylogenetic analyses were performed with a maximum likelihood approach (ML) (RAxML, ver. 8.2.12, see https://github.com/stamatak/standard-RAxML; Stamatakis 2014) and with Bayesian inference (BI) (MrBayes ver. 3.2.7, see https://nbisweden.github.io/MrBayes/download.html; Ronquist *et al*. 2012). *Nymphon australe* and *Austropallene cornigera* were chosen as outgroups, as both genera have been found to be closely related to *Pallenella* (Ballesteros *et al*. 2020). Their sequences were downloaded from GenBank (Table 1).

Seven different matrices were analysed with both approaches: *COI*-only, *ITS*-only without masking, *ITS*-only with masking using threshold ‘2’, *ITS*-only with masking using threshold ‘5’, *COI*+*ITS*-combined without masking, *COI*+*ITS*-combined with masking using threshold ‘2’, and *COI*+*ITS*-combined with masking using threshold ‘5’. Combined matrices were always portioned by gene fragment. Bayesian analyses were run for 50 × 10^6 generations with ‘nruns = 4’ and ‘nchains = 6’, saving every 5000th tree, the first 10% of retained trees were discarded as burn-in. The best-fitting evolutionary model had been determined in MEGA (ver. 10, see https://www.megasoftware.net/; Kumar *et al*. 2018) following the AIC criterion. GTR+I+Γ was suggested and employed as the evolutionary model. In the *ITS*-only analyses, the ingroup was forced to be monophyletic to ascertain that the two outgroup sequences were not placed within the ingroup. RAxML was run under the GTR+Γ model (–m GTRGAMMA), as inclusion of the invariant sites correction I is discouraged in combination with Γ in RAxML. Tree searching and bootstrapping was performed in a single run (–f a), using 1000 bootstrap replicates. The resulting trees were visualised with FigTree (ver. 1.4.3, see http://tree.bio.ed.ac.uk/software/figtree/) and their layout further modified in Adobe Illustrator. All phylogenetic analyses were computed on the CIPRES Science Gateway.

The ABGD analysis with *COI* was performed on the ABGD website (https://bioinfo.mnhn.fr/abi/public/abgd/abgdweb.html). In other studies on pycnogonids, ABGD has proved the most conservative of several distance-based approaches to species delimitation (Dietz *et al*. 2015*a*; Harder *et al*. 2016; Dömel *et al*. 2017) and was thus given preference to prevent overestimation of separate lineages. P_{min} and P_{max} were set to 0.01 and 0.1 respectively, whereas the number of steps was set to 100 and the relative gap width to 0.5. P_{min} and P_{max} represent the lowest and highest *p*-distance thresholds considered in the analysis (i.e. 1 and 10% respectively) whereas the relative gap width defines the minimum gap width percentage between putative species. Uncorrected *p*-distances, computed with MEGA (ver. 10) by pairwise deletion of gaps, were used as input. In the case of the *ITS* fragment, several poorly aligned regions with many indels

impeded assessing meaningful genetic distances. Masking and removing these indel-rich stretches removes the most variable regions, which would greatly distort any derived genetic distances, as only the more conserved regions are retained. To circumvent this problem, we computed *ITS* alignments for two groups of particularly closely related *Pallenella* forms, which were in the focus of our species delimitation efforts. The resulting alignments feature only few, well defined indels so that meaningful uncorrected *p*-distances could be calculated. Indels are considered neither in the distance calculation nor in the phylogenetic analyses; however, they account for part of the observed genetic differences between the different forms studied. To visualise these, we computed a median-joining haplotype network based on the *ITS* alignment for the '*variabilis*' complex morphotypes + *P. flava* with Network (ver. 5.0.1.1, Fluxus Technologies), which treats indels as mutational events.

Results

Collection success and assignment of field labels

Preliminary sorting in the field indicated that the 2015 material included five *Pallenella* species previously reported from the same locality. In addition, specimens of the two '*variabilis*' complex morphotypes 'black tips' and 'stripes' were recollected (Fig. 1) and three previously unknown *Pallenella* forms were segregated under field labels based on their size, live colouration and first inspection with low-magnification stereomicroscopy (Fig. 2). One of the new forms was provisionally designated as *Pallenella* cf. *ambigua* (Fig. 2*B*, *C*), owing to its resemblance to *Pallenella ambigua* (Stock, 1956), a large and predominantly yellow species (Staples 1997, 2014*a*). The two other new forms could not be assigned to a species based on field observation alone and were labelled 'pale green' and 'concentric bands' according to their colouration patterns (Fig. 2*D–I*).

Analysis of the mitochondrial COI fragment

The *COI* fragment could be successfully amplified for 17 of 20 *Pallenella* specimens selected from the 2015 material (Table 1). The fragment has a length of 657 bp in all cases except for specimens of *P.* cf. *ambigua* ($n = 3$), which feature a 12-bp insert (i.e. fragment length 669 bp: Supplementary file 2). As in our previous study (Arango and Brenneis 2013), amplification of *COI* for *Pallenella reflexa* (Stock, 1968) and *Pallenella pachycheira* (Haswell, 1884) proved challenging and was similarly difficult for *P.* cf. *ambigua*. For the latter two forms, clean sequences were obtained after cloning ($n = 2$ and 3 respectively). For *P. reflexa*, a clean *COI* fragment of 595 bp length was amplified with specifically designed nested primers ($n = 1$) (Table 2). In total, *COI* sequences of 40 *Pallenella* specimens comprised the final dataset (Table 1).

The *COI* analyses confirmed the morphological segregation performed in the field. Uncorrected pairwise *p*-distances between different forms range from minimally 3.3–3.7% to maximally 16.6–17.7%, whereas ingroup distances (for forms represented by more than one individual) are with 0–0.9% consistently low (Table 3). Analysis of the *COI* alignment by ABGD resulted in a step-wise decreasing number of groups with increasing threshold setting for the ingroup

Table 3. Uncorrected *p*-distances for the *COI* sequences of all *Pallenella* specimens studied

In-group distances are shown in bold. *n*, number of specimens per species

Pallenella species (field label)	*n*	*flava*	*constricta*	*baroni* (black tips)	*tasmania*	*reflexa*	*gracilis*	*brevicephala*	*pachycheira*	cf. *chevron* (stripes)	*harrisi*	cf. *ambigua*	*inflata*	*karenae* (conc. bands)	*laevis* (pale green)
flava	5	**0.0–0.9**													
constricta	3	10.8–11.4	**0.0–0.2**												
baroni, sp. nov. (black tips)	4	9.1–9.7	10.8–11.7	**0.0–0.8**											
tasmania	5	12.5–13.2	9.4–10.2	12.5–12.6	**0.0–0.2**										
reflexa	1	14.8–15.5	14.0–14.8	13.9–14.1	15.0–15.1	–									
gracilis	1	12.2–12.8	12.1–12.5	10.7–11.1	13.2–13.4	14.3	–								
brevicephala	5	13.4–13.9	12.6–12.9	13.1–13.7	14.2–14.5	16.8	12.9–13.2	**0.0–0.2**							
pachycheira	2	14.2–14.6	14.1–15.2	13.3–13.5	13.1–13.6	16.6–16.7	14.9–15.1	14.5–14.6	**0.3**						
cf. *chevron* (stripes)	5	8.2–9.0	10.6–11.9	3.3–3.7	12.3–12.6	13.6–13.8	11.7–11.9	13.2–13.5	13.4–13.5	**0.0–0.2**					
harrisi	1	10.8–11.3	10.8–11.4	10.2.-10.5	12.6–12.8	13.9	13.5	13.7	14.8–14.9	10.7–10.8	–				
cf. *ambigua*	3	10.7–13.2	10.3–11.3	11.3–12.6	12.2–13.1	14.1–15.0	14.6–15.4	14.0–14.6	14.3–15.4	11.6–12.8	4.7–5.9	**0**			
inflata	1	12.9–13.1	11.1–11.9	10.4–10.7	13.1–13.2	15.6	10.8	11.6–11.7	12.8–12.9	11.6	13.1	12.9–13.7	–		
karenae, sp. nov. (concentric bands)	1	13.4–13.7	11.9–12.8	12.0–12.2	13.5–13.7	14.8	12.9	11.3–11.4	12.2–12.3	12.5	14.6	14.9–15.7	9.3	–	
laevis (pale green)	3	16.6–17.7	14.2–15.2	15.4–15.7	13.5–13.7	15	14.5–14.8	15.1–15.4	16.4–16.9	15.1–15.2	16.3–16.6	16.3–17.2	15.8–16.3	14.9–15.1	**0.5–0.8**

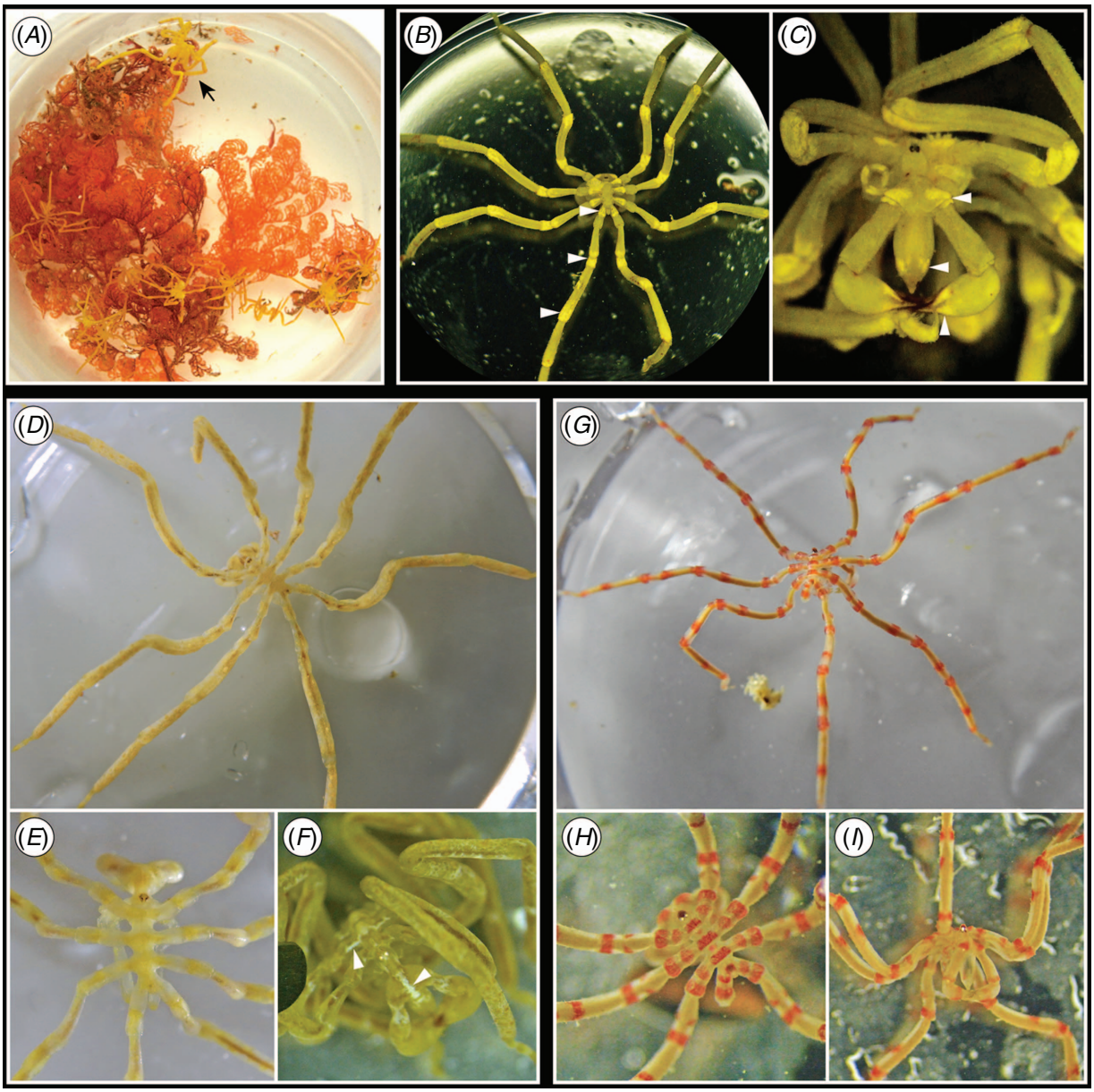

Fig. 2. Live specimens of new Tasmanian *Pallenella* forms. (*A*) Sample of various yellow as well as light orange *Pallenella* forms among arborescent bryozoans. Arrow points at a larger and more robust *P*. cf. *ambigua* specimen. (*B*, *C*) *P*. cf. *ambigua*, male. Arrowheads highlight regions and bands of more intense yellow colour. (*B*) Dorsal view. (*C*) Anterior aspect. (*D–F*) *P. laevis* ('pale green' morphotype). (*D*) Dorsal view of a female (17a). (*E*) Dorsal aspect of male (EN31). (*F*) Anterodorsal aspect of female (17a). Arrowheads point at white marks on cephalon and trunk. (*G–I*) *P. karenae*, sp. nov. ('concentric rings' morphotype), subadult female (EN15). (*G*) Dorsal view. (*H*) Dorsal aspect of trunk and proximal leg articles. (*I*) Anterolateral aspect.

distance *p*. Fourteen *Pallenella* groups are recovered under $0.2\% \leq p < 3.4\%$, corresponding to all morphologically segregated species and morphotypes. In the range of $3.4\% \leq p < 4.7\%$, the two morphotypes 'black tips' and 'stripes' collapse into one group, whereas further increase of *p* leads to merging of *P. harrisi* with *P*. cf. *ambigua*.

Concurrent with the distance-based approaches, ML- and BI-based phylogenetic analyses resulted in congruent topologies in which the different species and morphotypes are recovered as separate clades with unambiguous support (Fig. 3). The two pairings that proved threshold-sensitive in the ABGD analysis are here recovered as sister taxa respectively, with the shortest between-group branch lengths.

Analysis of the nuclear ITS *fragment and comparison to* COI *results*

The *ITS* fragment could be amplified for all 20 *Pallenella* individuals selected from the 2015 material (Table 1). Its length varies from 1058 to 1148 bp between the different

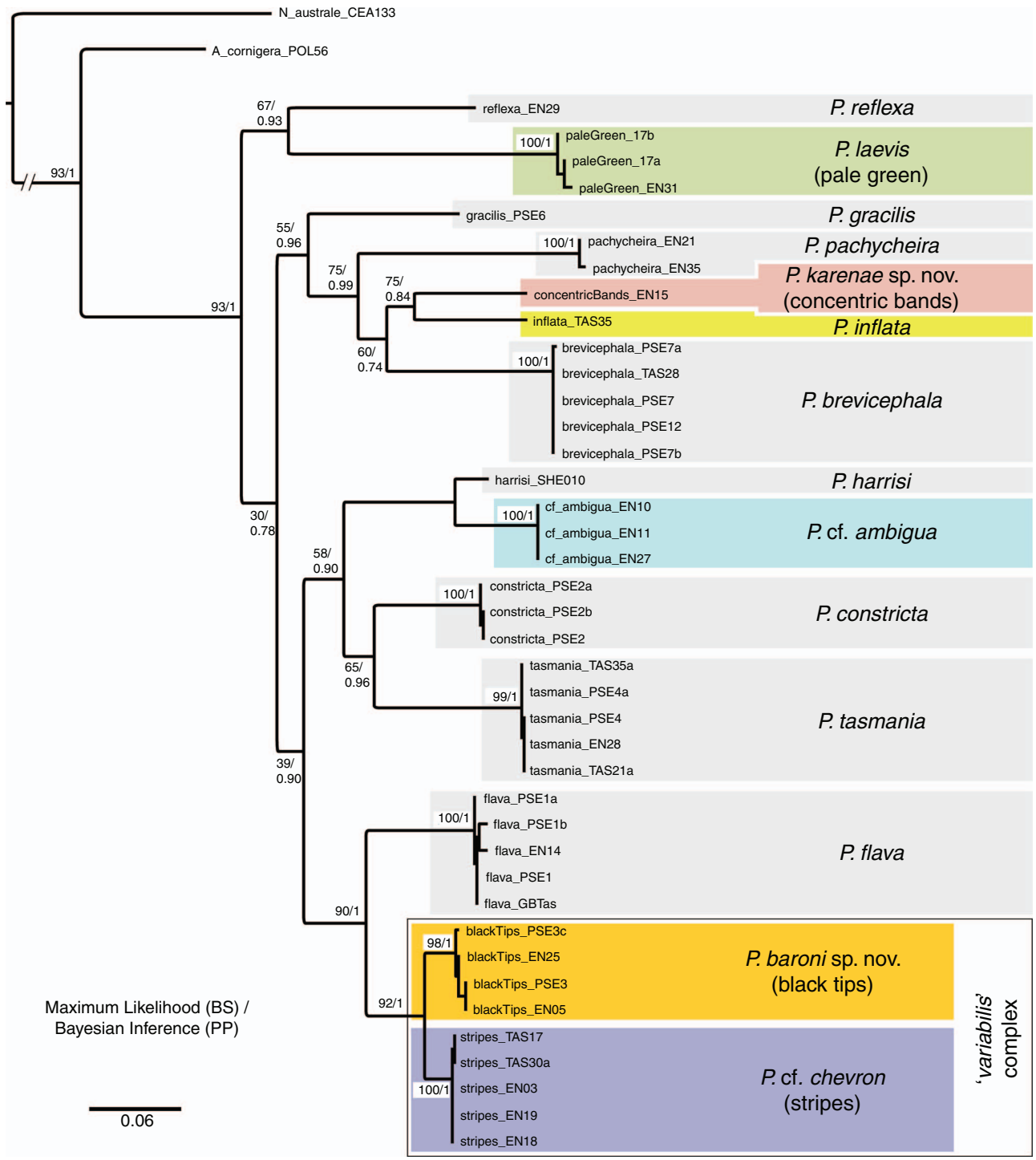

Fig. 3. Phylogenetic analysis of the mitochondrial *COI* fragment. The phylogram is based on the ML analysis; BI resulted in the same tree topology. Bootstrap support (BS) and posterior probability (PP) are shown for each node. Previously described *Pallenella* species are shown on light grey background. New forms are highlighted in colour. For interpretation of the references to colour in this figure legend, the reader is referred to the online version of this article.

species and morphotypes. These differences are due to the considerably variable *ITS1* and *ITS2* regions (Supplementary files 3–5). In total, 42 *Pallenella* specimens were included in the final *ITS* dataset (Table 1).

Similar to *COI*, phylogenetic analyses of the nuclear *ITS* fragment resulted in congruent topologies under ML and BI approaches, showing strong support for monophyletic species and morphotypes regardless of masking regime (Fig. 4). The

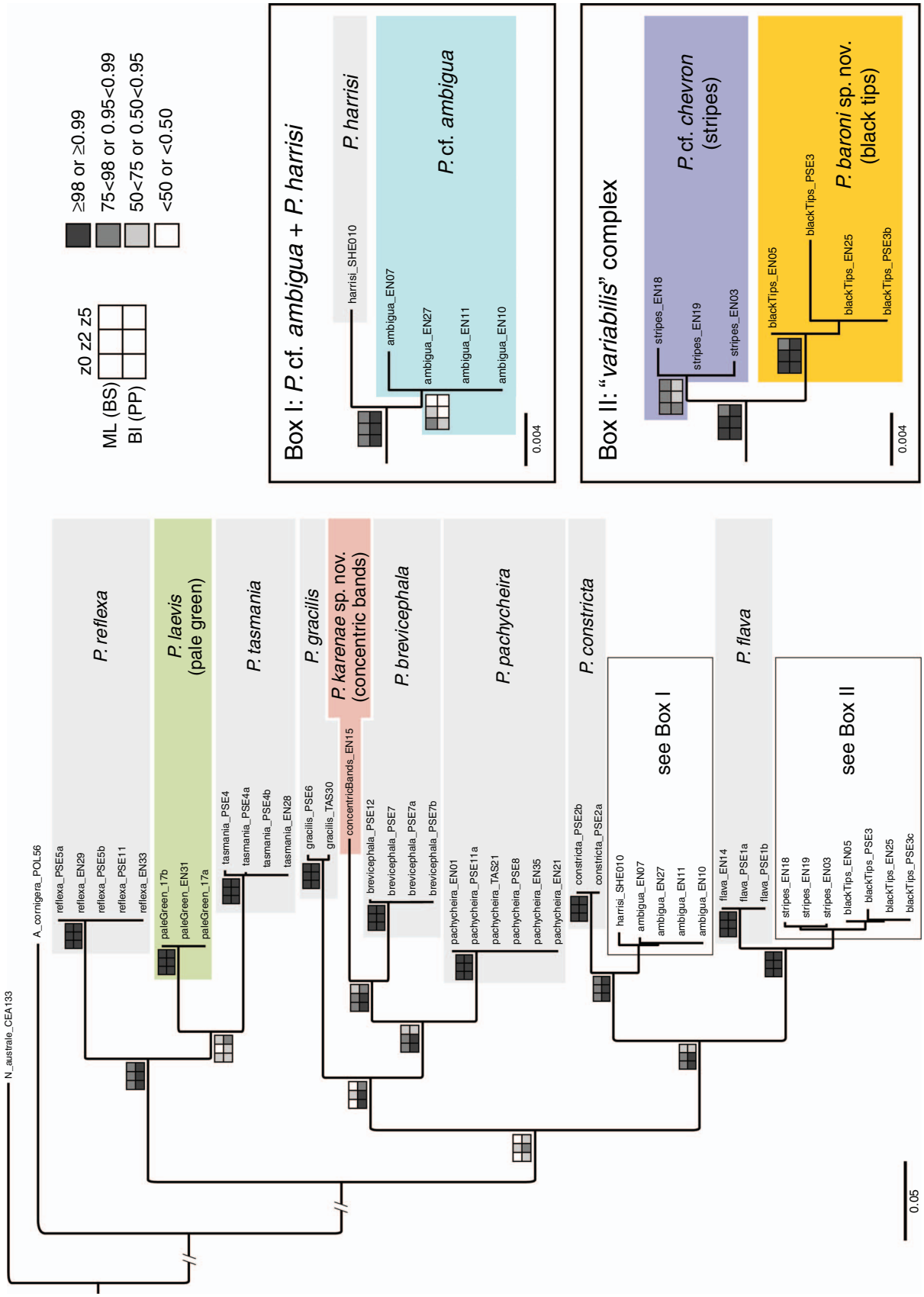

Fig. 4. Phylogenetic analysis of the nuclear *ITS* fragment. The phylogram is based on the ML analysis without masking. The tree topologies were identical in all other analyses. Bootstrap support (BS) and posterior probability (PP) under the different masking regimes (none = z0; zorro '2' = z2; zorro '5' = z5) are indicated at each node according to the legend in the top right corner. Previously described *Pallenella* species are shown on light grey background. New forms are highlighted in colour. In boxes I and II, clades of closely related forms are shown in more detail. For interpretation of the references to colour in this figure legend, the reader is referred to the online version of this article.

only cases in which masking-induced changes of support occur are (1) a clade comprising *P. harrisi* and *P.* cf. *ambigua* and (2) a clade containing the two '*variabilis*' morphotypes (see boxes I and II in Fig. 4). Both cases are evaluated separately (see below).

Beyond the good agreement of the *COI* and *ITS* results at species and morphotype level, the overall topologies for both gene fragments are also remarkably similar, indicative of a largely concurrent phylogenetic signal in both markers for the genus *Pallenella* (compare Fig. 3 and 4; but note deterioration of support at deeper nodes). Only *Pallenella tasmania* (Arango & Brenneis, 2013) is unstable when comparing *COI* and *ITS* topologies (sister clade to *Pallenella constricta* (Arango & Brenneis, 2013) in *COI v.* sister clade to 'pale green' morphotype in *ITS*). Accordingly, combined analyses of *COI* and *ITS* also recovered a largely congruent topology in which all 13 *Pallenella* forms included receive unambiguous support across all settings (Fig. S2). *P. tasmania* is here consistently recovered in a lineage together with *P. reflexa* and the 'pale green' morphotype, but interrelationships of the three taxa and their support differ depending on masking and reconstruction method. In general, the combined analyses point to four major lineages within *Pallenella*, which had also been recovered in the *ITS*-only analyses. These lineages are: (A) *reflexa* + *tasmania* + 'pale green', (B) *gracilis* + *pachycheira* + *brevicephala* + 'concentric bands', (C) *constricta* + *harrisi* + cf. *ambigua*, and (D) *flava* + 'black tips' + 'stripes'. Whereas support for a clade comprising lineages C and D is strong, its relationship to lineages A and B is unstable (Fig. S2).

Genetic and morphological delineation of 'pale green' and 'concentric bands' morphotypes

Based on *COI p*-distances (Table 3), ABGD analysis and phylogenetic analyses of *COI* and *ITS* (Fig. 3, 4), the new morphotype 'pale green' is found to belong to a species previously undocumented from the area. In line with this, detailed morphological investigation of the three individuals revealed a unique combination of traits that distinguish them from all congeners from Tasmanian waters. These include moderately inflated trunk segments and a short, upward-inclined anal tubercle, a markedly bulbous chela palm with relatively delicate and sharply pointed fingers and a curved propodus with characteristic heel spine pattern (Fig. 7). Notably, all of these features show a striking resemblance to those observed in *Pallenella laevis* (Hoek 1881), the type species of the genus. Accordingly, the three 'pale green' specimens are assigned to this species.

Moreover, the 'concentric bands' specimen is clearly set apart from all other *Pallenella* forms in the *COI* and *ITS* analyses (Table 3; Fig. 3, 4). In addition to its distinctive live colouration (Fig. 2*G–I*), its morphology differs from that of all congeners previously recorded in Tasmanian waters or any other locality (Fig. 8). Morphologically closest to 'concentric bands' is *Pallenella inflata* (Staples 2005) (Fig. 9), which is also reflected in their reciprocally lowest *COI p*-distance (9.3%) in support of a relatively close relationship (Fig. 3). Both forms share inflated trunk segments and a semierect anal tubercle with *P. laevis*, but can be distinguished from the latter by their pronounced preocular mound with distinct cuticular division line as well as deviating proboscis, chela and propodus shapes. Delineation of *P. inflata* from 'concentric bands' is possible based on (1) the much more inflated segments of *P. inflata* (Fig. 9*D v.* 8*D*) and its taller ocular tubercle, (2) the lack of dorsal setae on the trunk segments of *P. inflata* (Fig. 9*E, F*) as opposed to a single mid-dorsal seta on trunk segments 2 and 3 (Fig. 8*B, B′*), and (3) a higher number of teeth along the margins of the elongate oviger claw in *P. inflata* (Fig. 9*G*) combined with an often rounded, scoop-shaped tip (Staples 2005, 2008), contrasting with the more acute tip of 'concentric bands' (Fig. 8*F′*). Further, the live Tasmanian *P. inflata* specimen studied here has not been reported to feature a conspicuous pattern of coloured bands, and also Staples (2005) does not report a striking colour pattern for his collected specimens. Based on the concordance of morphological and molecular data, the 'concentric bands' morphotype is therefore assigned to a new species, *Pallenella karenae*, sp. nov.

Genetic delineation of the 'stripes' and 'black tips' morphotypes

With the new material obtained in 2015, the 'stripes' and 'black tips' morphotypes were re-evaluated. For the genetic analyses, material consisted of specimens that were collected (1) in two different years ('black tips': 2009, 2015; 'stripes': 2007, 2015: Table 1) and (2) from two different diving spots in which both forms were found to occur next to each other.

The two morphotypes are well-supported separate clades in the *COI* analyses (Fig. 3). They represent sister clades with the least divergence of all *Pallenella* forms studied (3.3–3.7% distance: Table 3) and are accordingly the first two groups that collapse into one in AGBD (see above). Analysis of the *COI* alignment (Supplementary file 2) reveals 19 morphotype-specific single nucleotide substitutions separating the 'black tips' and 'stripes' specimens (n = 4 and 5 respectively). Two additional positions further distinguish the two morphotypes, but are also variable in at least one of them. None of these substitutions translate into amino acid sequence differences.

In the *ITS* analyses, both morphotypes are resolved as sister clades as well (see box II in Fig. 4). Support for the monophyly of 'black tips' is unambiguous across all alignments (BS > 99; PP = 1.0), except for a slight decrease in the ML analysis under the most rigorous masking (BS = 88). Monophyletic 'stripes' are also well supported in all three ML analyses (BS $\geq$ 89), whereas support varies slightly more across the BI analyses, being highest without masking (PP = 0.98) and lowest under a moderate masking regime (PP = 0.80).

To exclude loss of signal due to potential misalignment of informative sites or masking in the complete *ITS* dataset, we scrutinised an unambiguous alignment comprising only the *ITS* sequences of 'black tips' and 'stripes' (n = 4 and 3 respectively) and their presumably closest relative *Pallenella flava* (Arango & Brenneis, 2013) (Supplementary file 6). Here, both forms can be distinguished based on seven morphotype-specific nucleotide substitutions and additionally on a deletion of three nucleotides unique to the 'black tips' specimens (position 301–303 in Supplementary file 6). Accordingly,

visualisation in an *ITS* network of the three *Pallenella* forms shows 'black tips' and 'stripes' separated by 10 mutations, with 'stripes' being more similar to *P. flava* (Fig. 5).

Morphological investigation of the 'stripes' and 'black tips' morphotypes

With the exception of their distinctive live colouration, the 'stripes' and 'black tips' morphotypes are more similar to each other than to any of the other Tasmanian *Pallenella* forms. Hence, identification of morphological traits distinguishing them proved challenging ('black tips': $n_{ad} = 9$, $n_{subad} = 5$; 'stripes': $n_{ad} = 4$, $n_{subad} = 5$). Both forms share (1) a bullet-shaped proboscis without any constrictions, (2) a shallow, evenly rounded preocular mound lacking a cuticular division line, (3) non-inflated, glabrous trunk segments with only few minute setae dorso-distally on the lateral processes, (4) a slightly swollen horizontal anal tubercle that overreaches leg process 4 at least minimally, and (5) marginally curved propodi with inconspicuous heel bearing a linear row of proximo-distally increasing spines followed by a pair of smaller spines (Fig. 10, 11). Although the adult 'stripes' specimens studied are slightly larger than the majority of adult 'black tips', one male specimen of the latter was found to fall well within the range of the 'stripes' (Fig. S1*C*).

In taxonomic studies of *Pallenella*, countable characters, such as the compound spines on oviger articles 7–10, small teeth along the margins of the oviger claw, and propodus heel spines are commonly evaluated for their potential for species delimitation. In all three traits, the subadult and adult 'stripes' specimens display, on average, higher values than their 'black tips' counterparts, but the respective ranges of the two morphotypes overlap (Fig. S1*D–F*). Further, in both morphotypes, the number of oviger and propodus spines increases distinctly from subadults to adults (Fig. S1*D*, *F*). Corresponding to this ontogenetic trend, also regenerating smaller legs display lower heel spine numbers than full-grown legs in the same specimen (not shown).

Principal component analysis (PCA) of relative measurements was performed separately for subadults and adults. In subadults, the first and second principal components (PC1 and PC2 respectively), explained 58.9 and 25.9% of the variation in the complete variable set, compared with 56.5 and 30.3% in the reduced set. Irrespective of dataset, both morphotypes are distinctly separated along PC1 (Fig. 6*A*), with chela, ocular tubercle, propodus and main claw measurements contributing most to its loading. In the PCA of adults, the first two PCs explained 42.6 and 18.1% of the variation in the complete dataset compared to 43.7 and 21.6% in the reduced one, but did not separate the morphotypes (Fig. 6*A′*), and neither did any of the lower-ranked PCs (not shown).

Initial investigation and measurements suggested that the cheliphore is proportionately larger in 'stripes' than in 'black tips' specimens. Further, chela shape was observed to differ: 'black tips' invariably feature an elongate chela with moderately inflated palm (Fig. 10*A–A‴*, *D*, S3*C*, *D*), whereas the chela of 'stripes' specimens tends to be slightly more compact and more bulbous (Fig. 11*B–C″*, S3*C′*,*D′*). Plotting of relative chela length and relative palm depth over body length indicates a decrease of both values with increasing body size, as opposed to a constant plateau (Fig. 6*B*, *C*). A corresponding slight decrease could be observed for relative scape length (data not shown). This suggests allometric growth in subadult and adult stages of both morphotypes, with a more pronounced size increase of the trunk compared to the size and volume of the cheliphores. If assuming a linear relationship (a simplification, as moulting does not lead to continuous size changes), 'stripes' specimens are indicated to have a proportionately longer chela as well as a proportionately more voluminous palm than 'black tips' specimens of the same body length (Fig. 6*B*, *C*).

Additional morphometric differences were reliably present in subadults of both forms, but more variable in the adults. The ratio of chela length and height (=measure for chela elongation) is higher in 'black tips' than in 'stripes' subadults (>2 and <2 respectively), whereas such a clear difference is not present in adults (Fig. 6*D*, S3*C–D′*). The same holds for the ratio of ocular tubercle height and width (=measure for tubercle 'tallness'), which is consistently lower in 'stripes' than in 'black tips' subadults, whereas it varies in adults (Fig. 6*E*, S3*A*,*A′*). This increased variation from subadult to adult stages is also reflected in a relatively low, and in some cases, even statistically non-significant correlation of both values with body length (Fig. 6*D*, *E*).

Comparison of the Tasmanian P. *cf.* ambigua *with the* P. ambigua *holotype*

Specimens of *P.* cf. *ambigua* ($n_{ad} = 6$, $n_{subad} = 4$) were compared with the male *P. ambigua* holotype. Morphological

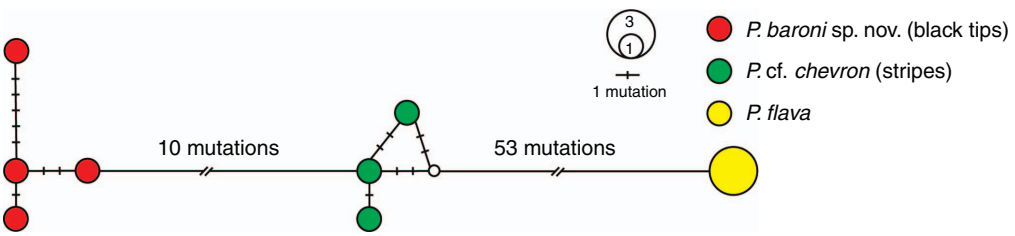

Fig. 5. *ITS* haplotype network of *Pallenella* cf. *chevron* ('stripes') and *P. baroni*, sp. nov. ('black tips') together with *P. flava* (Arango & Brenneis, 2013). *P. baroni*, sp. nov. specimens (red) cluster separately from *P.* cf. *chevron* specimens (green), which are in turn distinct from *P. flava* (yellow). For interpretation of the references to colour in this figure legend, the reader is referred to the online version of this article.

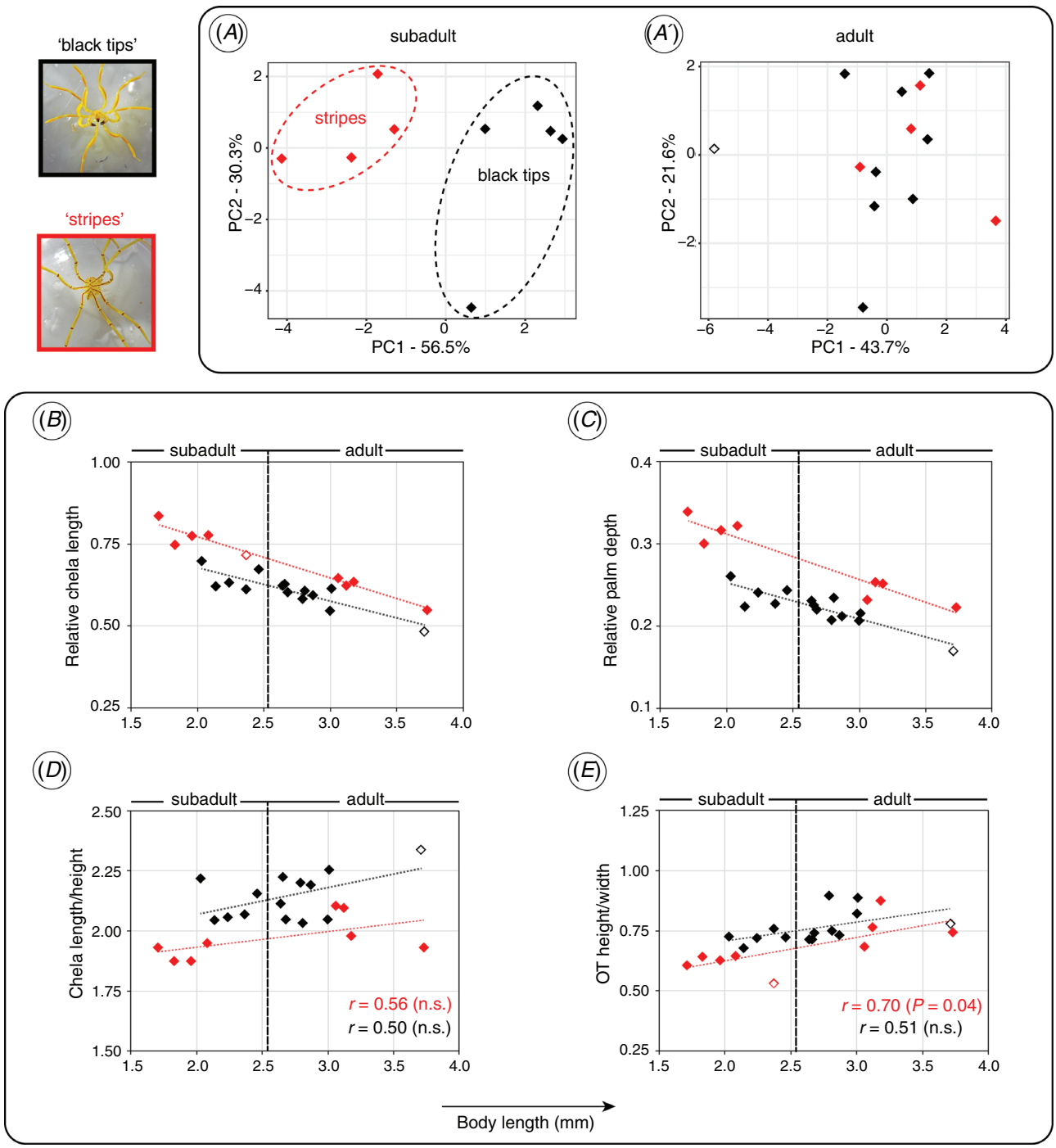

Fig. 6. Principal component analysis and selected measurements of *Pallenella baroni*, sp. nov. ('black tips') and *P.* cf. *chevron* ('stripes') specimens. *P. baroni*, sp. nov. shown as black diamonds, *P.* cf. *chevron* as red diamonds. Open diamonds indicate freshly moulted specimens. (*A*, *A*′) Plots of PC2 over PC1 obtained from PCA of reduced dataset of relative measurements. (*A*) Subadults. *A*′, Adults. (*B–E*) Plots of different relative measures or proportions over body length, including subadults and adults. Pearson correlation coefficient and p-values indicated for both morphotypes (n.s., non-significant). (*B*) Relative chela length. (*C*) Relative palm depth. (*D*) Ratio chela length/height. (*E*) Ratio ocular tubercle (OT) height/width. For interpretation of the references to colour in this figure legend, the reader is referred to the online version of this article.

correspondences are striking, including large body size, proboscis shape, curvature of the chela fingers, oviger claw, leg proportions, propodus shape and heel spine arrangement (Fig. 12). Further, the Tasmanian specimens show a yellow body colouration when alive (Fig. 2*A–C*), which is also reported for *P. ambigua* from Victoria (near Bass Strait, the type locality of the species: Staples 1997, 2014*a*). Few differences were apparent though. The holotype features a more pronounced neck

(Fig. 12*A*, *A*′, *C*, *C*′), its anal tubercle is slightly swollen at mid-point (Fig. 12*C*, *C*′), and the chela palm is more bulbous than in any of the Tasmanian specimens.

Comparison of P. *cf.* ambigua *with* P. harrisi

The *COI* and *ITS* analyses unequivocally set *P*. cf. *ambigua* apart from all other sympatric *Pallenella* forms. Rather, the allopatric *P. harrisi* from New South Wales is recovered as the genetically closest congener. Based on *COI*, segregation of both forms appears straightforward, featuring ~5% *p*-distance (Table 3), a unique insert of 12 nucleotides exclusively in *P*. cf. *ambigua* (Supplementary file 2), and unambiguous support (BS = 100; PP = 1) for monophyly of the latter in the phylogenetic analyses (Fig. 3). However, representation of *P. harrisi* by a single specimen in the sequence analyses impedes testing reciprocal monophyly. The *ITS* analyses recovered good support for *P. harrisi* + *P*. cf. *ambigua*, regardless of masking (BS $\geq$ 92; PP = 1), but monophyletic *P*. cf. *ambigua* received only moderate support (BS = 72; PP = 54) when no masking was applied (see box I in Fig. 4). To exclude potential loss of informative sequence stretches in the *ITS* alignment of all species and morphotypes, unmasked sequences of *P. harrisi* and the *P*. cf. *ambigua* were separately aligned and analysed (Supplementary file 7). Even in this unambiguous alignment, *p*-distances between the two allopatric forms lie below 1%. Contrary to this, distinction between live specimens is readily done, as *P. harrisi* has a dark red body colouration overlain by a pattern of conspicuous yellow marks and concentric bands (Fig. 13*A*′). A corresponding pattern of yellow bands and marks is evident on *P*. cf. *ambigua*, even though they are more difficult to discern against the underlying pale yellow colouration of body and appendages (Fig. 2*B*, *C*, 13*A*). Morphologically, both forms (and the *P. ambigua* holotype) are very similar and show only few differences. The few *P. harrisi* specimens studied (n_{ad} = 1, n_{subad} = 2) have a proportionately shorter scape and a more inflated chela palm (Fig. 13*B*, *B*′) and exceed *P*. cf. *ambigua* in chela height and robustness of the fingers (Fig. 13*C*, *C*′). These differences result in an even more compact and massive appearance of *P. harrisi* in anterior view (Fig. 13*B*, *B*′).

Discussion

Suitability of COI *and* ITS *for species delimitation in Pycnogonida*

The current study expands the set of available *COI* and *ITS* sequences for the diverse Australian *Pallenella* forms and thus allows a more comprehensive approach to the taxonomy of this genus than previously possible (Arango and Brenneis 2013). Our analysis of the mitochondrial *COI* fragment recovered 14 lineages within *Pallenella* that are concurrent with morphologically well-defined species and field morphotypes. The genetic distances between the different *COI* clades are in most cases pronounced (~10% and higher) and threshold-based delineation of groups by ABGD was unambiguous for 10 of the 14 *Pallenella* lineages, including the rediscovered *P. laevis* and the new species *P. karenae*, sp. nov.

Apart from our previous work on *Pallenella* (Arango and Brenneis 2013), the mitochondrial 'barcoding' gene *COI* (Hebert *et al*. 2003) has been used in biogeographic studies of several sub-Antarctic and Antarctic pycnogonid taxa with broad distribution ranges and pronounced morphological variation. Whereas differentiation into separated *COI* lineages was found to be surprisingly low in some cases (e.g. *Nymphon australe*: Mahon *et al*. 2008; Arango *et al*. 2011; Soler-Membrives *et al*. 2017), other studies recovered several distinct *COI* lineages suggestive of overlooked species diversity (e.g. *Pallenopsis patagonica* complex: Weis *et al*. 2014; Harder *et al*. 2016; Dömel *et al*. 2017; *Colossendeis megalonyx* complex: Krabbe *et al*. 2010; Dietz *et al*. 2013). Notably, subsequent analysis of *COI* together with *ITS* revealed incongruences between mitochondrial and nuclear signal content in the *C. megalonyx* complex (Dietz *et al*. 2015*a*). This indicated overestimation of species numbers when relying on *COI* alone. On the other hand, such mito-nuclear discordances between both markers were not observed in another colossendeid complex nor in the *P. patagonica* complex (Dietz *et al*. 2015*b*; Dömel *et al*. 2017) and the concordance in both markers strengthened support for the delineated *COI* clades as isolated evolutionary lineages. In the meantime, the findings for the *P. patagonica* and *C. megalonyx* complexes have been largely confirmed and further refined with a more comprehensive phylogenomic approach coupled to morphological investigation (Dömel *et al*. 2019, 2020).

In our study, inclusion of the nuclear *ITS* marker revealed strong mito-nuclear concordance and agreement with morphology at species level in *Pallenella*. This corroborates previous work examining the general suitability of these two gene fragments for taxonomic studies in this genus (Arango and Brenneis 2013). Notably, the divergence of the four major lineages in *Pallenella* that we recovered in our phylogenetic analyses has been recently indicated to date back to the Cretaceous (Ballesteros *et al*. 2020). Such a comparably old age of the genus' initial radiation may account for the clear-cut results not only in the fast-evolving *COI* fragment but also in *ITS*. At the same time, however, this supposedly late Mesozoic radiation of *Pallenella* highlights a remarkably slow rate of morphological change in the genus.

First new record of the 140-year-old type species and reinstatement of the genus name Pallenella

Prior to this study, *Pallenella laevis* was known only by its holotype, an adult female from Bass Strait (Hoek 1881). Although no genetic data are available for the holotype, its original description and a recent morphological reinvestigation (Staples 2014*a*) reveals sufficiently strong similarities to the Tasmanian 'pale green' specimens (voucher # QMS111240) to assign them to *P. laevis* with high confidence. After nearly 150 years, this is only the second documented record of the species (first record from Tasmanian waters) and we here provide the first live observation data, a redescription of a well preserved adult female as well as notes on deviating male features (see Systematics section: Fig. 7).

Not least due to damage and suboptimal preservation of the holotype (see Staples 2014*a*), *P. laevis* has undergone a taxonomic odyssey. The original description assigned it to the genus *Pallene* (Hoek 1881), erroneously describing it with a two-articled scape. This misleading feature led to its first separation into the monotypic genus *Pallenella* (Schimkewitsch 1909), only to be synonymised with *Pseudopallene* a century later (Staples 2005). At that time, *Pseudopallene* encompassed Northern and Southern Hemisphere species with strongly developed, ventrally directed cheliphores and a lack of palps. In a recent revision of *Pseudopallene*, Staples (2014*a*) proposed the new genus *Meridionale* that groups the Southern Hemisphere forms, with Hoek's *laevis* specimen as type species. However, the reinstatement of the *laevis* specimen as type species calls for the resurrection of the original genus name. In spite of Schimkewitsch (1909) erecting *Pallenella* based on an invalid diagnostic character, his genus name takes precedence over *Meridionale*. A recent phylogenomic study of pycnogonid relationships (Ballesteros *et al*. 2020) supports the validity of the morphology-based separation of genera proposed by Staples (2014*a*), recovering monophyletic *Pallenella* and suggesting *Pseudopallene* to be more closely related to the genus *Austropallene* Hodgson, 1915.

Genetic analyses support separation of 'black tips' and 'stripes' into two species

Re-evaluating the status of the morphologically similar 'black tips' and 'stripes' morphotypes was one of the main aims of the current study. In previous analyses, their close relationship was already indicated, but lack of genetic replication within morphotypes impeded definitive conclusions (Arango and Brenneis 2013). Here, our expanded *COI* dataset resolves both forms as strongly supported sister clades. However, the comparably low *COI p*-distances of 3.3–3.7% stands in contrast to most of the other *Pallenella* forms and renders delimitation of both lineages threshold-sensitive in the ABGD analysis. Nonetheless, such low interspecific distance values are not unprecedented for pycnogonids, and have been previously reported for closely related congeners of the genus *Pallenopsis* (Dömel *et al*. 2017, 2019). Concomitantly, separate analysis of the nuclear *ITS* fragment argues in favour of a separation of 'black tips' and 'stripes' into independently evolving units, rather than only into different mitochondrial lineages. In addition to their reciprocal monophyly and the presence of several diagnostic nucleotide substitutions and deletions in both markers, the two morphotypes also satisfy the criterion of sympatry that has been found crucial for species delimitation under the biological species concept (Schwentner *et al*. 2011; Kekkonen and Hebert 2014). Both morphotypes not only occur in the same geographic area, but have been found side by side at the same diving locations. The material sampled for genetic analyses was specifically selected to include such sites. Based on our results, we thus conclude that 'black tips' and 'stripes' are reproductively isolated biological species.

Pending further analyses, we designate the Tasmanian 'stripes' form as *P*. cf. *chevron* (see Systematics section: Fig. 11). To date, very few specimens of *P. chevron* (Staples, 2007) have been described from South and Western Australia (Staples 2007; Arango 2009), with considerable morphological similarities to the two Tasmanian forms studied here. Crucially, this species has been reported to feature longitudinal stripes and a V-shaped dorsal chevron mark on the trunk segments (Staples 2007), which we confirmed based on holotype photographs. However, genetic data are still missing for South or Western Australian specimens. In contrast to *P*. cf. *chevron*, the 'black tips' morphotype is assigned to the new species *Pallenella baroni*, sp. nov. (see Systematics section: Fig. 10).

Live colouration matters – delineation of P. *cf.* chevron *and* P. baroni, *sp. nov. in the field*

In the field, specimens of *P. baroni*, sp. nov. and *P*. cf. *chevron* were correctly segregated based on their live colouration pattern. Owing to the distinctive red lines on body and appendages, *P*. cf. *chevron* conspicuously stands out from all other congeners in the area. Despite some variation in intensity and stripe extensions, a stable core pattern is present in all specimens (Fig. 2*D–D″*, 11*A–A″*; see Systematics section) including adults, subadults and also late postlarval instars (PS6 *sensu* Brenneis *et al*. 2011*b*) (Fig. S3*B′*, *F*, *G*). Also a freshly moulted subadult (EN03) and an adult kept alive for 24 days in captivity and without access to fresh bryozoans retained the pattern (not shown). This speaks for persistence of the red marks throughout (late) ontogeny and independently of specific physiological states, such as nutrition level or intermoult period. Together with our genetic results, this supports the previous suggestion that such marks can serve as a diagnostic character for *Pallenella* species (Staples 2007). Inconveniently, however, long-term fixation of the pattern depends crucially on the preservative used. It persists (at least for several years) as long as material is kept in high-percentage ethanol (>95%) and, to a lesser extent, also in formaldehyde containing fixative (compare Fig. 11*A*, *A′ v.* 11*A″*). Storage in lower-percentage ethanol (70–80%) frequently leads to a loss of the marks, highlighting the need for documentation of live colouration of newly collected specimens.

In contrast, the 'black tips' of *P. baroni*, sp. nov. are not preservation-sensitive – but nor are they diagnostic. In the *Pallenella* material studied, a variable dark crust on proboscis and chela fingers is a consistent feature of *P. baroni*, sp. nov., but was also found on single specimens of *P*. cf. *chevron* (Fig. S3*A′*, *C′*, *D′*, *E*), *P. inflata* (Fig. 9*A–C*) and *P. pachycheira*. Moreover, the presence of such dark marks on the chela fingers has been previously reported for *P. ambigua* (Staples 1997). Hence, in spite of having been introduced as a field label for *P. baroni*, sp. nov. (Arango and Brenneis 2013), the black tips do not suffice for reliable species identification and need to be considered in combination with additional morphological features. Incidentally, one *P. baroni*, sp. nov. adult appeared to have freshly moulted and lacked the dark crust completely (Fig. 10*A″*), otherwise showing all 'typical' characteristics (plain yellow body colouration, elongate and moderately inflated palm, three propodus heel spines on all legs and low oviger spine number despite large

body size). This suggests acquisition of the crust over time, potentially as a result of crushing and feeding on a chemically defending bryozoan prey species.

Same but different – morphological delineation P. *cf.* chevron *and* P. baroni*, sp. nov.*

When excluding live colouration, morphological delineation of *P*. cf. *chevron* and *P. baroni*, sp. nov. remains challenging. In spite of trends in the countable characters (e.g. oviger compound spines, propodus heel spines), intraspecific variation results in overlapping ranges. This impedes use of these characters for reliable diagnosis. Further, our morphometric analyses indicate proportional changes of body regions during ontogeny of *Pallenella*. Although previous studies already noted this phenomenon, they referred predominantly to earlier postembryonic or juvenile instars in comparison with adults (Stock 1956; Staples 2005, 2008; Brenneis *et al*. 2011*b*), as opposed to the more advanced subadult stages considered here. Beyond this, we also found indications for allometric growth during adulthood, which – if confirmed by investigation of more material – renders morphometric distinction even more challenging. Although studies on moulting in sexually mature *Pallenella* are pending, it is known to occur in some other sea spiders, such as *Pycnogonum litorale* (Strøm, 1762), a long-lived species that can be kept under laboratory conditions (Meyer and Bückmann 1963; Lotz and Bückmann 1968). Interestingly, the 2015 material encompassed some large adult *Pallenella* with very soft and clean cuticle, pristine setae without traces of wear, and some legs partially still stuck in an exuvia. These findings speak in favour of adult moults in *Pallenella*, thus making continuing allometric growth a feasible cause for size-dependent shifts of body proportions. This could partly explain why a previous cluster analysis including morphometric data failed to recover *P*. cf. *chevron* as a separate group among other Tasmanian congeners (Stevenson 2003). In our analyses, adults of *P*. cf. *chevron* feature a larger chela with a more bulbous palm, if compared with similarly sized *P. baroni*, sp. nov. However, these differences are slight and embedded in the background of intraspecifically more variable features (e.g. chela heights, anal tubercle length), which may account for the lack of separation in our plots of the first factors in the adult PCA. In contrast, the separation of subadults by PCA confirmed our impression that morphological delimitation of subadult stages is more straightforward. Nonetheless, we caution that the comparably low sample size (especially for adult *P*. cf. *chevron*) calls for additional sampling to ascertain the consistency of our findings.

Same or different? – the ambiguous case of P. *cf.* ambigua*,* P. ambigua *and* P. harrisi

Although the presence of *P. ambigua* in Tasmanian waters has been mentioned before (Clark 1963; Staples 2014*a*), the species identity of Tasmanian material has never been confirmed, largely due to the bewildering diversity of 'yellow' sea spiders in the area. The similarities between the large *P*. cf. *ambigua* in our 2015 material and the holotype of *P. ambigua* and specimens from the coast off Victoria are striking (Stock 1956; Staples 2005, 2014*a*; Arango and Brenneis 2013) and their close affinity is beyond doubt. However, as no DNA data are available for non-Tasmanian specimens, we opt to retain *P*. cf. *ambigua* under investigation, pending morphological and genetic analyses with additional material.

The same considerations hold for *P. harrisi* from New South Wales. Although the *COI* data indicate ~5% divergence from *P*. cf. *ambigua*, their marginal differentiation based on *ITS* and the lack of replication to assess reciprocal monophyly of the two allopatric forms preclude definitive conclusions. Notably, the corresponding pattern of yellow bands found in *P*. cf. *ambigua* further underlines their similarities (live specimens), despite a different general body colouration. It remains to be tested whether the proportional differences of the cheliphore are a variable feature of a single widespread species or rather a diagnostic character for closely related species along the south-eastern coast of Australia.

The more the merrier: unprecedented sympatric diversity in Tasmanian Pallenella

Prior to this study, seven sympatric species of *Pallenella* were described from south-east Tasmania, excluding the two morphotypes of the unresolved '*variabilis*' complex (Arango and Brenneis 2013). Additionally, some reports suggested the presence of *P. ambigua* in the area, but it either remained questionable whether this species was truly found (Stevenson 2003) or no detailed descriptions were provided (Clark 1963; Staples 2014*a*). Here, we present evidence for no less than 13 sympatric *Pallenella* species in the coastal waters off south-east Tasmania, exceeding the hitherto documented diversity of this genus in any other location (Staples 2005, 2007, 2008, 2014*a*). A comparably high sympatric species richness in a single genus has been rarely reported for Pycnogonida, and concentration of so many congeners within a few kilometres of coastline in seemingly identical microhabitats on a single prey type is – to our knowledge – unprecedented. For instance, the genus *Anoplodactylus* (Phoxichilidiidae) has been shown to be represented by 15 species in tropical shallow waters of Colombia (Müller and Krapp 2009), but samples were collected from various habitats with different (potential) prey groups (e.g. hydrozoans, bryozoans, algae). Further examples of corresponding sympatric species richness may be found in the genera *Ammothea* (Ammotheidae) and *Nymphon* (Nymphonidae) from Antarctic waters (e.g. Munilla and Soler-Membrives 2009). In these cases, however, documentation of stable co-occurrence of species in the same microhabitat of a small study area is hampered by geographic remoteness and accessibility.

Even in south-east Tasmania, it remains unknown whether all 13 *Pallenella* species are represented by stable long-term populations. Pycnogonids are generally considered 'crawlers' and 'brooders' with limited dispersal potential (e.g. Griffiths *et al*. 2011, Soler-Membrives *et al*. 2017). Dispersal may be even more restricted in species featuring large lecithotrophic hatching stages that stay attached to the father for part of the postembryonic development, as found in Callipallenidae and several other families (Brenneis *et al*. 2017; Brenneis and Arango 2019). However, some sea spiders have been reported

to possess limited swimming capability, including *Pallenella* (Morgan 1977; Staples 2014*a*, 2014*b*), and others have been found 'piggybacking' on medusae through the pelagial (Pagès *et al*. 2007). Accordingly, it is possible that ovigerous males drift in the water column and set up a new population where they settle. However, if the locality is not favourable for long-term establishment – for instance due to strong interspecific competition with congeners – it may remain temporary. Contrary to the latter notion, our repeated collections in the same area over several years as well as previous reports (Stevenson 2003) and the extensive local taxonomic knowledge (Karen Gowlett-Holmes, pers. comm.) support persistence and co-occurrence of several of the *Pallenella* species in Tasmanian waters for more than a decade.

Possible reasons for this exceptionally high sympatric diversity of *Pallenella* along the Tasmanian coast and the ecological segregation of the different species are largely unexplored. Their (apparently) obligatory association with arborescent bryozoans calls for more detailed documentation of the prey species in order to obtain insights into specificity of predator–prey interactions (Staples 1997). The differences of chela and proboscis shapes between several sympatric congeners may point to a preference of different *Orthoscuticella* prey species. Although collection of more than one *Pallenella* species from the same bryozoan colony seems to speak against this, the mere presence of a pycnogonid in a bryozoan does not *per se* prove a predator–prey-relationship. Therefore, actual feeding needs to be unequivocally documented in future studies – *in situ* as well as in controlled experiments. Further, the identified prey bryozoans have to be subjected to a corresponding integrative taxonomic analysis. Notably, some Australian pycnogonids appear to use sequestered alkaloids taken up from chemically defending bryozoan prey as an antipredator defence, e.g. against fish (Blackman and Walls 1995; Sherwood *et al*. 1998). For instance, specimens at the time considered as *P. ambigua* were found to contain increased levels of the alkaloid norharman, potentially derived from harman produced by their bryozoan prey *Orthoscuticella ventricosa* (Blackman and Walls 1995). Further, high concentrations of alkaloids from the bryozoan *Amathia wilsoni* were detected in a species of *Stylopallene*, which in turn was encountered in significantly higher numbers than any other sympatric pycnogonid (including *Pallenella*) on this bryozoan species (Sherwood *et al*. 1998). The latter finding is suggestive of species-specific tolerances for the defensive compounds of bryozoans – which may be one of the factors contributing to the ecological segregation of different *Pallenella* species. Accordingly, it seems possible that a chemical arms-race between predator and prey may act as a driver of prey specialisation, ecological segregation and potentially even speciation in this and other pycnogonid genera.

Outlook

Our study of *Pallenella* from the south-eastern tip of Tasmania provides a sound basis for future investigations seeking to unravel the taxonomy, biogeography and evolutionary history of this colourful sea spider genus across its entire distribution. With more systematic sampling, further increases of species numbers can be almost taken for granted. For instance, the two non-Tasmanian forms of the provisional '*variabilis*' complex (Arango and Brenneis 2013) clearly suggest the existence of widespread *Pallenella* species complexes of multiple similar congeners in Australian waters. It remains to be tested whether *COI* and *ITS* alone will enable confident species delineation once more allopatric forms are included in the analyses. Recent studies of the Antarctic and sub-Antarctic *Pallenopsis patagonica* and *Colossendeis megalonyx* complexes have shown that further extension of population genetic datasets may be needed for reliable delimitation of closely related allopatric congeners (Dömel *et al*. 2019, 2020), as well as precise estimation of such phenomena as gene flow, introgression, and lineage sorting between recently diverged sympatric species.

Systematics

Callipallenidae Hilton, 1942

Pallenella Schimkewitsch, 1909

All specimens investigated fall into the resurrected genus *Pallenella* Schimkewitsch, 1909. Prior to the current study, the exclusively Southern Hemispheric *Pallenella* encompassed 15 species (Bamber *et al*. 2020). However, one of these species – *Pallenella dubia* (Clark, 1963) – remains currently listed as *taxon inquirendum*, as Clark's specimens are juvenile instars that have not yet attained (sub)adult morphology, rendering unequivocal species identification challenging (Staples 2014*a*). For this reason, *P. dubia* has been omitted from the following morphological species identification key for adults. Further, because of remaining ambiguities pertaining to geographic and intraspecific variability of morphological characters (other than live colouration) in *P.* (cf.) *ambigua* and *P. harrisi*, both forms are not distinguished in the key.

Key to *Pallenella* species (adults)

1a. Long leg articles (femur, tibiae 1&2) each with two distinct annular constrictions; chela with bulbous palm and robust fingers ..... ***P. pachycheira*** (Haswell, 1884)
b. Long leg articles without distinct annular constrictions 2
2a. Curved propodus with prominent heel and paired spines arranged in V-shape; long leg articles with slightly irregular, undulating surface ..... ***P. reflexa*** (Stock, 1968)
b. Heel spine arrangement different; long leg articles with smooth surface 3
3a. Proboscis with marked constriction at $^{1}/_{2}$–$^{2}/_{3}$ of its length, distal part bulbous, tapering sharply towards jaws; curved propodus with pronounced heel bearing linear array of stout spines ..... ***P. constricta*** (Arango & Brenneis, 2013)
b. Combination of characters different 4
4a. Neck region minimal (just constriction next to ocular tubercle); distinct preocular longitudinal division line; propodal heel with 7–10 well developed but short spines, laterally flanked by several smaller ones ..... ***P. brevicephala*** (Staples, 2008)
b. Combination of characters different 5

5a. Neck region very short (less than diameter of oviger base); no preocular longitudinal division line; proboscis with slight constriction at mid-length; propodus almost straight with inconspicuous heel bearing linear array of spines increasing in size from proximal to distal, high oviger spine count (≥60) ..... ***P. tasmania*** (Arango & Brenneis, 2013)

b. Combination of characters different 6

6a. Chela fingers short and robust, ~$^{1}/_{4}$ of palm length, with blunt tips and prominent lobe on cutting edge; low preocular mid-dorsal mound with longitudinal division line; proboscis with subterminal fringe of setae..... ***P. watsonae*** (Staples, 2005)

b. Combination of characters different 7

7a. Acute preocular mid-dorsal mound; trunk segments dorso-ventrally inflated; anal tubercle inclined upwards; propodus moderately curved with inconspicuous heel.....8

b. Combination of characters different 10

8a. Longitudinal division line only anteriorly, not extending across preocular mound; chela fingers with delicate pointy tips; anal tubercle inflated; trunk segments 2 and 3 dorsally with multiple tiny setae in unordered array..... ***P. gracilis*** (Arango & Brenneis, 2013)

b. Distinct longitudinal division line across preocular mound; anal tubercle not inflated; trunk segments 2 and 3 dorsally glabrous or each with one mid-dorsal seta 9

9a. Trunk segments strongly inflated; segments 2 and 3 dorsally glabrous; oviger claw with elongate tip that may be rounded (scoop-shaped)..... ***P. inflata*** (Staples, 2005)

b. Trunk segments moderately inflated; segments 2 and 3 each with a single short mid-dorsal seta; oviger claw shorter with acute tip..... ***P. karenae***, sp. nov.

10a. No preocular longitudinal division line; trunk segments moderately inflated and dorsally glabrous; anal tubercle inclined upwards; chela palm bulbous; curved propodus with prominent heel bearing linear array of spines, high oviger compound spine count (≥60) ..... ***P. laevis*** (Hoek, 1881)

b. Character combination different 11

11a. Preocular cephalon evenly rounded with longitudinal division line at anterior base; chela with markedly inflated palm and robust fingers; proboscis with slight constrictions at $^{1}/_{3}$ and $^{2}/_{3}$ of its length..... ***P.* (cf.) *ambigua*** (Stock, 1956) & ***P. harrisi*** (Arango & Brenneis, 2013)

b. Preocular cephalon without longitudinal division line 12

12a. Basal $^{2}/_{3}$ of proboscis almost cylindrical, distal $^{1}/_{3}$ narrowing sharply to short tube-shaped end; propodus distinctly curved with heel spines in non-linear array..... ***P. difficile*** (Arango, 2009)

b. Character combination different 13

13a. Body length ≥4 mm; preocular cephalon evenly rounded; proboscis marginally inflated at mid-length; horizontal anal tubercle as long as lateral process of trunk segment 4; long leg articles robust, tibia 2 approximately twice as thick as tarsus and propodus, leg length >18 mm; no dark pigmentation marks on trunk segments or legs ..... ***P. flava*** (Arango & Brenneis, 2013)

b. Body length <4 mm; preocular cephalon evenly rounded or with hint of acute mid-dorsal mound; proboscis bullet-shaped; horizontal anal tubercle overreaching lateral process of trunk segment 4 at least minimally; long leg articles slender, tibia 2 less than twice as thick as tarsus and propodus, leg length typically <18 mm 14

14a. Majority of legs with 4 or more major heel spines in linear array, distally followed by smaller heel spine pair; at least weak red-brownish dorsal chevron marks on trunk segments and stripes on legs; leg length can be >18 mm ..... ***P.* (cf.) *chevron*** (Staples, 2007)

b. Majority of legs with 3 major heel spines in linear array, distally followed by smaller spine pair; chela elongate (length : height ≥2) with moderately inflated palm (chela length : palm depth ≥2.5); no signs of chevron marks or stripes; proboscis tip and chela fingers typically covered with dark crust; leg length <18 mm..... ***P. baroni***, sp. nov.

Pallenella laevis (Hoek, 1881)

(Fig. 2*D–F*, 7)

Pallene laevis Hoek, 1881: 78–79, pl. 11, fig. 8–12.
Parapallene laevis Loman 1908: 46–47.
Pallenella laevis Schimkewitsch, 1909: 7.
Pseudopallene laevis Staples, 2005: 159–60.
Meridionale laevis Staples, 2014: 348–50, fig. 3*a–e*.

Material examined

QM S111240, 1 female (17a [DNA voucher]), 2 males (17b, EN31 [both DNA vouchers]), 30 Oct. 2015, Cathedral in Waterfall Bay, Eaglehawk Neck, Tasmania, 10–20-m depth.

Description of female (17a)

Live colouration: pale green and semitransparent, dark midgut diverticula discernible through cuticle, inconspicuous white marks form a longitudinal dorsal line on cephalon, transverse lines on the anterior side of the lateral processes and more irregular patterns on appendages. Neither greenish colour nor white marks persist after preservation in PFA/SW or in ethanol.

Body: fully segmented, glabrous but for scattered tiny setae distally on lateral processes, segments dorsally and ventrally rounded, lateral processes 1.75–2 times as long as wide at their base, separated by almost their own basal diameter when live, but only about half their diameter after PFA/SW fixation, presumably owing to contraction of the longitudinal intersegmental musculature.

Cephalon: narrow neck as long as oviger base, prominent distal crop more than three times as wide as neck, shallow mid-dorsal preocular mound but no median cuticular division line.

Ocular tubercle: moderately tall, base wider than total height, angling slightly backwards, two pairs of eyes (pigmentation lost in PFA/SW fixation), anterior eye pair sitting slightly lower than posterior pair, a pair of apical papillae (=external protrusion of the lateral sense organ) dorsal to the eyes.

Proboscis: directed ventrally, slightly shorter than cheliphore scapes (when basal membrane retracted), proximal third widening slightly, then tapering very gradually, along distal third more rapidly towards the mouth opening, no setiferous fringe surrounding the mouth.

Cheliphore: well developed with functional chela and sparse tiny setae (only visible under stereomicroscope); scape one-articled with proximal constriction line, angling outwards from cephalon, slightly longer than proboscis; chela directed medially with considerably inflated palm; chela fingers with pointed tip, about one-third of palm length; immoveable finger's outer margin continues straight from palm with shallow bump halfway; moveable finger's outer margin evenly curved and minimally shorter than the immoveable finger, both finger's sclerotised cutting edges almost straight apart from very shallow proximal elevation on moveable finger, narrow gap between cutting edges when fingers closed.

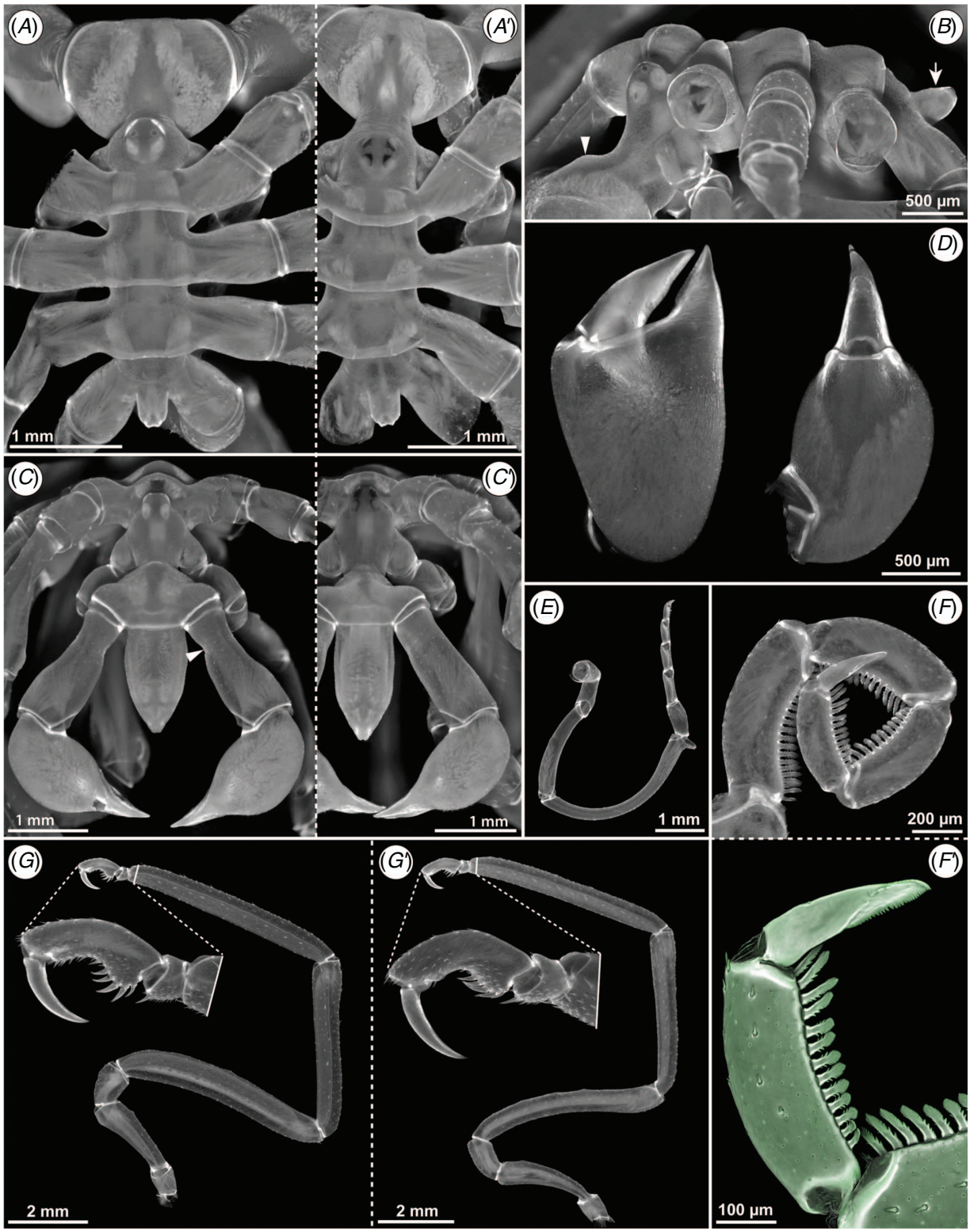

Fig. 7. *Pallenella laevis* (Hoek, 1881). Morphotype 'pale green'. (*A*) Dorsal aspect of female (17a). *A*′, Dorsal aspect of male (EN31). Note collapsed cuticle of trunk segments and lateral processes. (*B*) Lateral view of trunk (female, 17a). Note moderately inflated trunk segments, slightly elevated mid-dorsal mound on cephalon (arrowhead) and upwardly inclined anal tubercle (arrow). (*C*) Anterior view of female (17a). Note basal constriction of scapes (arrowhead). *C*′, Anterior view of male (EN31). (*D*) Right chela (female, 17a) in frontal and posterior view (left and right respectively). (*E*) Oviger of male (EN31), proximal article 1 missing. Note distinct distal apophysis on curved article 5. (*F*) Strigilis of female (17a). Note high number of >60 compound spines on articles 7–10. *F*′, Detail of oviger article 10 and oviger claw (cLSM scan). Note fine denticulation along the claw's margin and the tapering but not acutely pointed tip. (*G*) Leg of female (17a) with magnification of tarsus, propodus and main claw. Note prominent propodus heel and heel spines. *G*′, Leg of male (EN31) with magnification of tarsus, propodus and main claw. Note proportionately slightly longer coxa 2 and lower femur diameter.

Oviger: article 5 longest, marginally curved, without distal apophysis; compound spine formula 21 : 17 : 14 : 14 (right oviger); terminal claw two-thirds as long as article 10, tapering distally to narrow rounded tip, margins with minute teeth, especially on endal side.

Legs: macroscopically smooth surface, sparse cover of tiny setae visible under stereomicroscope; major articles laterally with visible longitudinal cuticular lines; coxa 2 three times as long as coxa 1; coxa 3 1.5 times as long as coxa 1; femur second longest article, thicker than tibiae, ventral surface marginally irregular because of minor elevations along the proximo-distal axis, oocytes visible through cuticle; tibia 2 longest article; tarsus short, one large tarsal spine aligned with propodal heel spines; propodus curved with prominent heel bearing 4–6 spines (varies between legs) whereof the spines in the middle are largest, propodal sole covered with numerous small spinules; main claw slender, evenly curved with sharp, pointed tip, about two-thirds of propodus length, tip meeting propodal heel spines when closed; auxiliary claws absent. Large ventral gonopore on the widened distal portion of coxa 2 of all legs.

Anal tubercle: distinctly shorter than lateral process of leg 4, semierect (i.e. ~45° upward inclination), without inflation, from mid-length on gradually narrowing towards tip with cleft anal opening, dorsally with sparse microscopic setae.

Measurements of female (mm)

Body length = 3.72; body width = 2.32; anal tubercle length = 0.33; ocular tubercle height = 0.30; proboscis length = 1.31; cheliphore scape = 1.55; chela length = 2.06; chela depth = 0.90; moveable chela finger = 0.88; oviger article 5 = 1.51, article 10 = 0.41, claw = 0.28; 3rd leg coxa 1 = 0.63, coxa 2 = 2.20, coxa 3 = 0.96, femur = 5.21, tibia 1 = 4.28, tibia 2 = 5.50, tarsus = 0.26, propodus = 1.01, claw = 0.65.

Description of males

Both males had a very soft cuticle, presumably because of a recent moult (right leg 1 of specimen 17b still stuck in leg exuvia). As a result, PFA/SW fixation (17b) as well as preservation in ethanol (EN31) resulted in partial collapse of leg articles and scapes and even of some trunk segments (due to contraction of longitudinal musculature, e.g. Fig. 7*A′*). Nonetheless, it is evident that the males correspond well to the female in overall size and most morphological details. Therefore, only significant deviations are listed:

Overall habitus slenderer than in the female. Lateral processes distinctly divided by their own proximal diameter or even more, still recognisable after fixation. Cephalon dorsally evenly rounded, lacking mid-dorsal mound. Scape without basal constriction line. Chela fingers leaving no gap when closed (17b) or a gradually increasing gap from the finger tips towards their bases (EN31). Oviger articles 4 and 5 evenly curved, article 5 distinctly longer than article 4, with apophysis at its distal end. Ovigeral compound spine formula 19 : 15 : 13 : 13 (17b, right oviger). Oviger claw only half as long as article 10. Femur marginally curved and slenderer than in female. Five propodus heel spines in most legs, specimen 17b with three spines on right leg 2 and left leg 1, and its right leg 1 stuck in moult (spine arrangement not discernible). Gonopore position not discernible with certainty as cuticle of coxae 2 collapsed.

Distribution

The new specimens from Eaglehawk Neck extend the known distribution range of *P. laevis* from Investigator Strait (South Australia) (Staples 2014*a*) across the type location Eastern Bass Strait (Hoek 1881) to the south-eastern tip of Tasmania.

Remarks

The specimens are in good agreement with the description of the female holotype by Hoek (1881). Further, Staples' (2014*a*) recent reinvestigation of the holotype using high-resolution stereomicroscopy leaves no doubt about the identity of the Tasmanian specimens. *P. laevis* is characterised by a unique combination of characters, which enable ready species diagnosis, including the strongly curved propodus with pronounced heel and linearly arranged long spines (differing from the more robust heel spines of *P. constricta*), the inflated trunk segments and semierect anal tubercle (shared only with *P. inflata*, *P. gracilis* and *P. karenae*, sp. nov.), the swollen chela palm with sharply pointed chela fingers and the high oviger compound spine count (60 spines or more, matched only by *P. tasmania*). In contrast, the width of a gap between the closed chela fingers and the presence of a shallow mid-dorsal preocular mound seem to be intraspecifically variable.

Live Tasmanian *P. laevis* specimens could be distinguished from congeners in the area by the naked eye because of their large overall size, relatively slender habitus and the pale greenish colouration with visible dark midgut diverticula.

In the literature, some uncertainty persists regarding the size of the holotype. Although Staples (2005) and Arango and Brenneis (2013) claimed it to be comparable in size to the large *P. ambigua* and *P. harrisi* with reference to the original description of Hoek (1881), Staples (2014*a*) correctly points out that Hoek's original body measurement (2.66 mm) lies considerably below the latter two species. However, Hoek's measurement of *P. laevis* leg length (21.5 mm) is very long and falls clearly into a similar range as the legs of *P. harrisi*, *P. ambigua* and the Tasmanian *P. laevis* specimens. The holotype's considerable leg length is also supported by the scale bars of the stereomicroscopic images of Staples (2014*a*), which at the same time indicate that its body length exceeds 3 mm – in agreement with the Tasmanian specimens. Taking into account that the holotype seems to exhibit a similar collapse of cuticular structures as observed by us during specimen fixation, the body length of the live *P. laevis* holotype may have been closer to 4 mm than to 3 mm. This makes it one of the largest but comparably more slender representatives of the genus, surpassed only by the more robust *P. ambigua* and *P. harrisi*.

Pallenella karenae, sp. nov.

(Fig. 2*G–I*, 8)

urn:lsid:zoobank.org:act:70414E8C-C659-44FA-A0DE-C48BAA8649CB

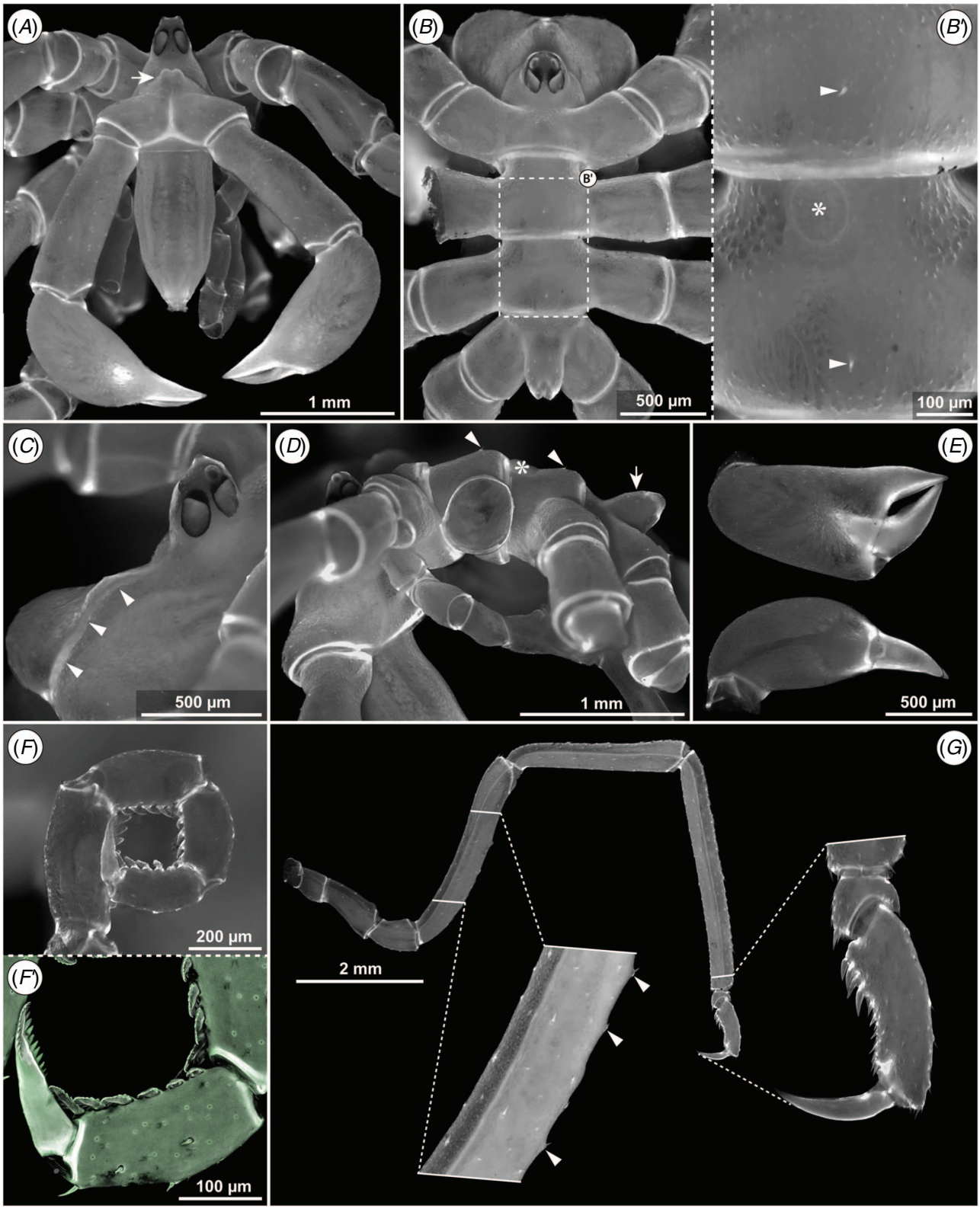

Fig. 8. Holotype of *Pallenella karenae*, sp. nov. Morphotype 'concentric bands', subadult female (EN15). (*A*) Anterior view. Note acute preocular mound (arrow). (*B*) Dorsal aspect. *B*′, Detail of trunk segments 2 and 3, dorsal view (area indicated by inset in *B*). Note single mid-dorsal seta on each segment (arrowheads). The asterisk marks an epibiont. (*C*) Detail of mid-dorsal mound and ocular tubercle. Note longitudinal division line extending across the mound (arrowheads). (*D*) Lateral view of trunk. Note moderate posterior inflation of the trunk segments, the mid-dorsal seta on segments 2 and 3 (arrowheads) and upwardly inclined anal tubercle (arrow). The asterisk marks an epibiont. (*E*) Right chela in frontal and posterior view (top and bottom respectively). (*F*) Strigilis (oviger articles 7–10). *F*′, Detail of oviger article 10 and oviger claw (cLSM scan). Note pointed tip of the claw and low number of prominent teeth along its margin. (*G*) Leg with magnification of tarsus, propodus and main claw (right) and a region of the femur. Note inconspicuous propodus heel with short spines as well as slightly elevated sockets (arrowheads) of setae on the long leg articles.

Material examined

(TMAG J6267): Holotype – 1 subadult female (EN15 [DNA voucher]), 28 Oct. 2015, Phoque Rock, Eaglehawk Neck, Tasmania, 13–17-m depth.

Diagnosis

Trunk glabrous and fully segmented, neck short, cephalon with acute preocular mid-dorsal mound and a distinct cuticular division line, trunk segments dorsally and ventrally with moderate inflation near the posterior margin, segments 2 and 3 bearing a single mid-dorsal seta, anal tubercle upward inclined in 45° angle, chela fingers less than half of palm length (about one-third of total chela length), moveable finger slightly shorter than immoveable one, legs without constrictions, propodus minimally curved with four short heel spines (less than half diameter of propodus), distinctive colouration pattern with red concentric bands when alive.

Description

Live colouration: cuticle transparent, yellow-orange midgut and its diverticula in cheliphore and legs clearly visible; distinctive pattern of transverse red bands on body and all appendages: some bands only dorsally (posteriorly on each trunk segment, at cheliphore base, on anal tubercle, distally on lateral processes and coxae 1), others concentric around distal podomere margins but often with ventrally fading intensity (scape, chela palm, coxa 3, femur, tibiae 1 and 2 and propodus); long leg articles with additional band at two-thirds of their length; coxa 2 with two lateral red patches; tip of ocular tubercle red; trunk segments 2 and 3 with additional antero-dorsal red patch; proboscis anteriorly with two longitudinal red lines. Colouration does not persist after fixation in ethanol.

Body: fully segmented, glabrous but for few microscopic setae on dorso-distal margin of lateral processes and one dorso-median seta on trunk segments 2 and 3, all segments dorsally and ventrally moderately inflated, lateral processes ~1.5 times as long as their basal diameter, separated by less than half of their own diameter.

Cephalon: neck short, expanding to distal crop almost directly anterior to oviger base, prominent preocular mid-dorsal mound and distinct median cuticular division line.

Ocular tubercle: prominent, as tall as base width, bent slightly backwards, two pairs of large eyes (pigmentation persists in ethanol), anterior eye pair sitting slightly lower than posterior pair, one pair of papillae (lateral sense organ) dorsal to eyes.

Proboscis: directed postero-ventrally, as long as cheliphore scapes, along proximal two-thirds almost parallel-sided, marginally dilated at about one-third of its total length, tapering along the distal third towards the tip, extended cuticular proboscis jaws form protruding circular rim around mouth opening, no setiferous fringe.

Cheliphore: well developed with functional chela, sparsely covered with microscopic simple setae; scape one-articled with hint of a proximal constriction line, as long as proboscis, angling outwards from cephalon; chela palm moderately swollen; each chela finger with sharply pointed tip, less than half of palm length, immoveable finger's outer margin curving only marginally towards moveable finger; moveable finger's outer margin evenly curved and slightly shorter than immovable finger, both fingers' inner cutting edges sclerotised and almost straight, only shallow bump halfway along moveable finger, prominent gap between cutting edges when finger tips touch.

Oviger: articles 4 and 5 subequal and longest, marginally curved, without distal apophysis; compound spine formula 12 : 6 : 6 : 6 (right oviger); terminal claw slender and tapering, more than half the length of article 10, margins bearing prominent blunt teeth, more pronounced and numerous (=11) on endal side.

Legs: sparsely covered by longitudinal rows of tiny setae on moderately elevated sockets, leading to rough appearance of cuticle surface; major articles with prominent longitudinal cuticle lines laterally; coxa 2 more than twice as long as coxa 1; coxa 3 1.5 times as long as coxa 1; femur second longest article, marginally curved, immature oocytes visible through cuticle; tibia 2 longest article; tarsus short, ventrally covered in small spinules, one more prominent median spine aligned with propodus heel; propodus only weakly curved with inconspicuous heel bearing four spines that gradually increase in size from proximal to distal but remain shorter than half of propodus diameter, propodal sole covered with numerous smaller spinules; main claw evenly curved with sharp, pointed tip, about two-thirds of propodus length; auxiliary claws absent. Gonopores not yet developed.

Anal tubercle: shorter than lateral process of leg 4, semierect (~45° inclined upwards), from mid-length onward tapering to tip with anal opening, dorsally with half a dozen scattered minute setae.

Measurements of female holotype (mm)

Body length = 2.40; body width = 1.45; anal tubercle length = 0.35; ocular tubercle height = 0.32; proboscis length = 1.19; cheliphore scape = 1.21; chela length = 1.40; chela depth = 0.54; moveable chela finger = 0.58; oviger article 5 = 0.65, article 10 = 0.22, claw = 0.17; 3rd leg coxa 1 = 0.45, coxa 2 = 1.04, coxa 3 = 0.60, femur = 2.88, tibia 1 = 2.09, tibia 2 = 3.60, tarsus = 0.15, propodus = 0.91, claw = 0.5.

Etymology

The new species is named after Karen Gowlett-Holmes, experienced diver, distinguished underwater photographer and marine invertebrates expert. Her knowledge of the local dive sites and help during the collection of Tasmanian *Pallenella* specimens contributed significantly to the success of the project.

Distribution

To date, the coastal waters near Eaglehawk Neck, Tasmania, are the only location in which *P. karenae*, sp. nov. has been reliably documented. However, live specimens with a strikingly similar colouration pattern have been observed in diving depths in Bass Strait (David Staples, pers. comm.), potentially indicating a wider distribution range of this new species. As of now, morphological and molecular study of Bass Strait specimens is pending.

Remarks

As the holotype is a subadult female, it is very likely that adults exceed it in size. Further, it cannot be excluded that some of the proportions of the appendage articles differ in adults. In particular, the oviger articles appear rather short for adult females of *Pallenella* and an increase in the oviger compound spine count seems likely in full-grown specimens.

The distinctive colouration pattern of live *P. karenae*, sp. nov. sets it clearly apart from most of its congeners. A comparable pattern with broad red bands is so far known only for a *Pallenella* form from New South Wales, which has been preliminarily placed in the partially unresolved '*variabilis*' complex (Arango and Brenneis 2013). However, in contrast to *P. karenae*, sp. nov., the bands of the New South Wales form are more numerous and narrowly spaced along the legs and its underlying general body colouration is bright yellow. Further, it is of distinctly larger size, lacks a preocular mound, inflated trunk segments and upward-inclined anal tubercle and differs in proboscis and chela shapes.

Pallenella inflata (Staples, 2005)

(Fig. 9)

Pseudopallene inflata Staples, 2005: 164, fig. 3*a–i*; 2008: 129–30, fig. 2*e, f*. *Meridionale inflata* Staples, 2014.

Material examined

QM S111241, 1 subadult (TAS35 [DNA voucher]), 26 Jan. 2007, Fortescue Bay, Eaglehawk Neck, Tasmania, 21-m depth.

Distribution

The subadult specimen studied extends the known distribution range of *P. inflata* from South Australia (Investigator Group Islands, Althorpe Islands) to the south-eastern tip of Tasmania.

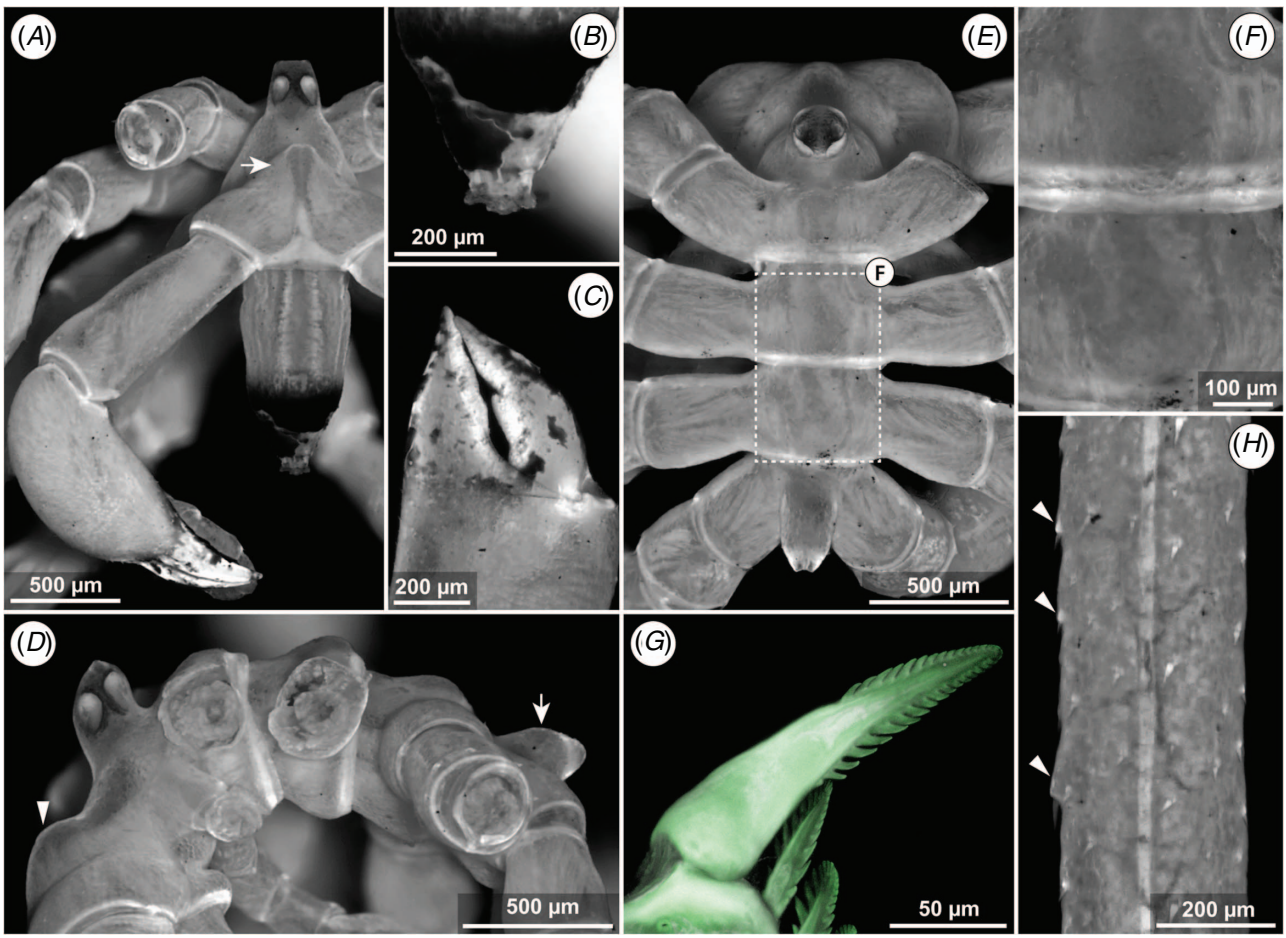

Fig. 9. *Pallenella inflata* (Staples, 2005). Subadult from Tasmania (TAS35). (*A*) Anterior view. Note acute preocular mound (arrow) and black marks on proboscis tip and chela fingers. (*B*) Proboscis tip. The extended jaws form a short tube protruding around the mouth. (*C*) Chela fingers. Moveable finger marginally shorter than its immoveable counterpart. (*D*) Lateral view of trunk. Note pronounced mid-dorsal mound on cephalon (arrowhead), tall ocular tubercle, pronounced inflation of the trunk segments and upwardly inclined anal tubercle (arrow). (*E*) Dorsal aspect. (*F*) Detail of trunk segments 2 and 3, dorsal view (area indicated by inset in *E*). Note complete lack of setae. (*G*) Detail of long, pointed oviger claw (cLSM scan). Note comparatively high number of teeth along both margins of the claw. (*H*) Detail of tibia 2. Note slightly elevated sockets of setae (arrowheads) and longitudinal cuticular ridge.

Remarks

Measurements of the subadult specimen (body length: 1.95 mm; leg length: 11.57 mm) show it to be slightly larger than the adult holotype from the Althorpe Islands (Staples 2005), possibly indicating size differences between different populations. The Tasmanian subadult falls into the same size range as the subadult of *P. karenae*, sp. nov., suggesting that body size alone is unsuitable for segregation of the two species.

The oviger compound spine count of the Tasmanian subadult (11 : 7 : 6 : 6) is likely to be higher in adults. The ovigeral claw does not show the scoop-shaped tip of the holotype but a more pointed one (Fig. 9*G*), which has also been noted for a specimen from the Investigator Group Islands (Staples 2008). As with several other Tasmanian congeners, the proboscis and chela tips of the *P. inflata* subadult are covered by a dark, flaky crust (Fig. 9*A–C*).

Pallenella baroni, sp. nov.

(Fig. 1*A–C*, 10, S3*A–D*)

urn:lsid:zoobank.org:act:7FBBA6FE-024F-4482-974B-0C0F29C7C137

Pseudopallene '*variabilis*' complex (plain yellow morphotype with dark tips of proboscis and cheliphores). Arango & Brenneis, 2013.
Meridionale '*variabilis*' complex. Staples, 2014.

Material examined

Holotype. TMAG J6268, 1 male (EN05 [DNA voucher]), 22. Oct 2015, Phoque Rock, Eaglehawk Neck, Tasmania, 13–17-m depth.

Paratypes. TMAG J6269, 1 female (EN25 [DNA voucher]), 30. Oct 2015, Cathedral in Waterfall Bay, Eaglehawk Neck, Tasmania, 18–21-m depth. QM S111242, 2 males (Exp4_1, Exp4_2), 2 females (5_1, 5_2), 22. Oct 2015, Phoque Rock, Eaglehawk Neck, Tasmania, 13–17-m depth. QM S92303, 1 female (PSE3), 1 male (PSE3a), 1 female (PSE3b) – collected in 2009, PSE3a&b DNA vouchers in Arango & Brenneis (2013). QM S111258, 1 subadult male (PSE3c) – collected in 2009, DNA voucher in Arango & Brenneis (2013). QM S111243, 2 subadult males (GBTAS_03&04); 2 subadults (GBTAS_05&06), 21.–24. Nov 2009, Phoque Rock, Eaglehawk Neck, Tasmania, 5–20-m depth.

Diagnosis

Trunk glabrous and fully segmented, trunk segments not inflated; cephalon with evenly rounded mid-dorsal mound lacking a longitudinal cuticular division line; anal tubercle slightly swollen around mid-length and overreaching lateral process of leg 4 at least minimally; proboscis bullet-shaped; chela of elongate shape (chela length ≥2 times chela height) with only moderately inflated palm (chela length ≥2.5 times palm depth); legs without constrictions and with sparse cover of simple setae; propodus marginally curved with inconspicuous heel bearing typically three major spines followed by a pair of smaller spines; live colouration plain yellow with slightly darker orange gut visible through cuticle.

Description of male holotype

Live colouration: yellow with orange gut visible through cuticle (intensity of colouration presumably depending on nutritional state); flaky, dark brownish crust covers distal third of proboscis (apart from its very tip) and chela fingers; yellow body colouration lost after preservation in ethanol but dark crust persists.

Body: fully segmented, glabrous but for few minute setae on dorso-distal margins of lateral processes, segments not inflated, lateral processes ~1.5 times as long as wide, separated by less than half their basal diameter.

Cephalon: neck as long as width of oviger base; distal crop about three times as wide as neck, with shallow and evenly rounded mid-dorsal mound, no median cuticular division line, right side partly covered by epibionts.

Ocular tubercle: moderately tall, slightly wider at base than high, anterior side sloping gradually down towards neck, anterior eye pair slightly lower than posterior pair, one pair of distinct apical papillae (=external protrusion of the lateral sense organ) dorsal to eyes.

Proboscis: directed ventrally, slightly shorter than cheliphore scape, bullet-shaped without constrictions, basal arthrodial membrane not extended, cuticular jaws open (giving impression of mammilliform tip), no setiferous fringe surrounding the mouth, flaky dark crust along distal third, epibionts covering part of proximal half.

Cheliphore: well developed with functional chela and sparse tiny setae (visible under stereomicroscope); scape one-articled, lacking proximal constriction, angling outwards from cephalon, chela directed medially with moderately inflated palm; chela fingers narrowing distally to pointed but not very sharp tips, slightly longer than half of palm length, covered in same flaky dark crust as proboscis; immoveable finger straight continuation of palm, only minimally curved; moveable finger curved along its proximal half and marginally shorter than the immoveable finger, cutting edges of both fingers strongly sclerotised, small protruding bump halfway along the edge of the moveable finger, wide gap between cutting edges when finger tips touch.

Oviger: article 5 longest with distal apophysis, article 4 second-longest, both curved along their length, compound spines on articles 7–10 : 16 : 12 : 10 : 11 (right oviger); terminal claw two-thirds as long as article 10, narrowing distally to rounded tip, distal margins lined by small teeth with tapering but not sharply pointed tips (12 on endal side).

Legs: sparse cover of small setae readily observable with low-magnification stereomicroscopy; major articles laterally with distinct longitudinal cuticular lines; coxa 2 three times as long as coxa 1 and 2.5 times as long as coxa 3; femur second longest article, slightly curved; tibia 2 longest article; tarsus short, one prominent tarsal spine aligned with propodus heel; propodus weakly curved with inconspicuous heel bearing three median spines (right leg 2 with four) that increase in size from proximal to distal, distalmost median spine longer than half of propodus width, followed by a pair of smaller spines, propodus sole covered with numerous tiny spinules; main claw evenly curved towards pointed tip, about two-thirds of propodus length; auxiliary claws absent; gonopores small, ventrodistally on coxa 2 of legs 3 and 4.

Anal tubercle: horizontal, marginally overreaching lateral process of leg 4, slightly swollen at midpoint, narrowing towards tip with cleft anal opening.

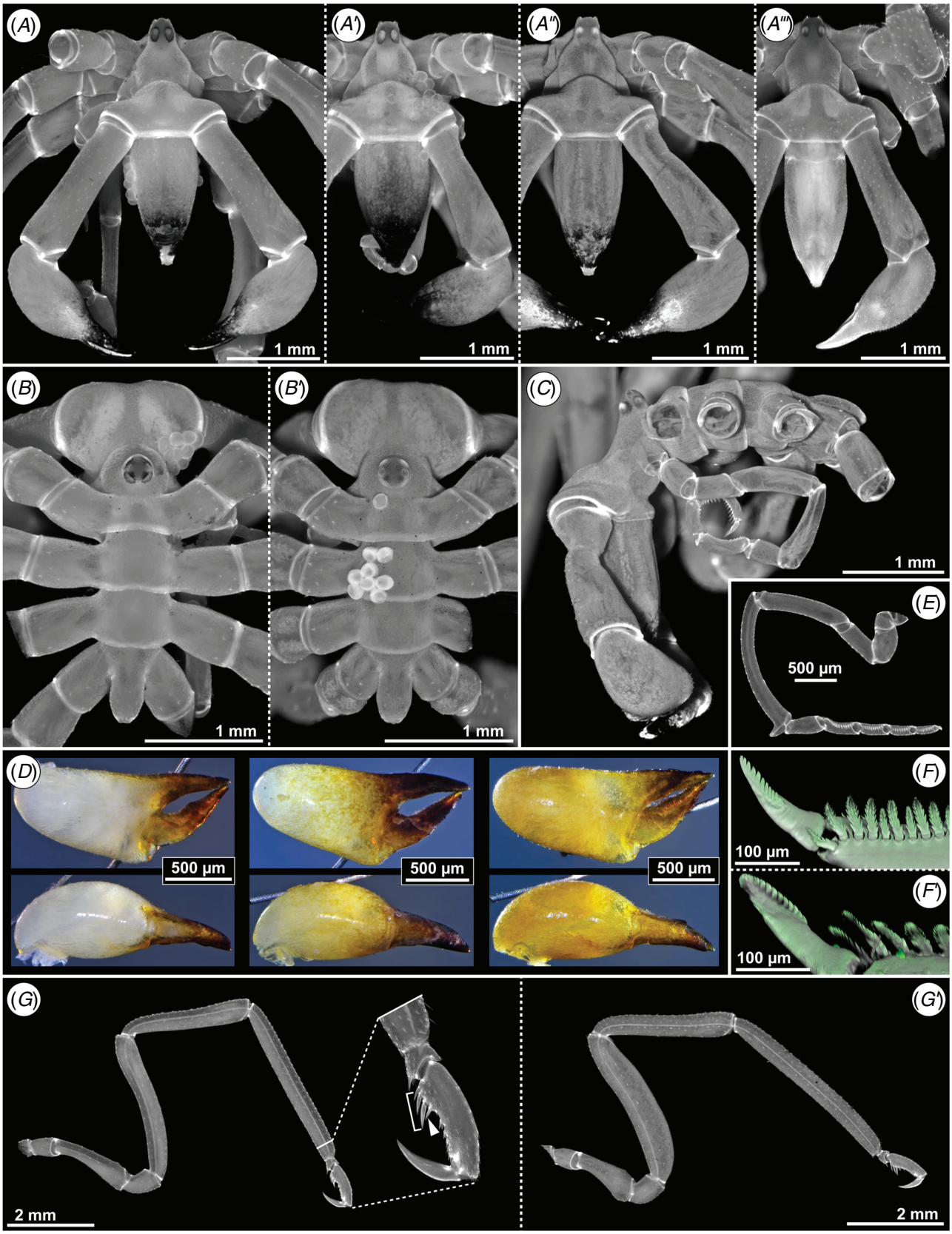
(A)
1 mm
(A')
1 mm
(A'')
1 mm
(A''')
1 mm
(B)
1 mm
(B')
1 mm
(C)
1 mm
(E)
500 µm
(D)
500 µm
500 µm
500 µm
(F)
100 µm
(F')
100 µm
(G)
2 mm
(G')
2 mm

Measurements of holotype male (mm)

Body length = 2.79; body width = 1.78; anal tubercle length = 0.4; ocular tubercle height = 0.26; proboscis length = 1.33; cheliphore scape = 1.55; chela length = 1.63; moveable chela finger = 0.73; oviger article 5 = 1.61, article 10 = 0.28, claw = 0.18; 3rd leg coxa 1 = 0.59, coxa 2 = 1.89, coxa 3 = 0.67, femur = 3.2, tibia 1 = 2.82, tibia 2 = 3.85, tarsus = 0.25, propodus = 0.93, claw = 0.57.

Description of female

All females studied resemble the males in overall size and most aspects of their morphology. Sex-specific divergent features: Scapes with more or less distinct proximal constriction; oviger articles 4 and 5 of subequal length, article 5 distinctly shorter than in male and without distal apophysis; coxa 2 proportionately shorter than in males, ~2.5 times as long as coxa 1 and twice as long as coxa 3; femur swollen, often mature oocytes dorsal to gut diverticulum visible through cuticle; all legs with large gonopore on ventro-distally swollen end of coxa 2.

Distribution

To date, *P. baroni*, sp. nov. has been documented from the coastal waters around Eaglehawk Neck, Tasmania.

Etymology

The new species is named after Mick Baron, who helped us during all collection trips at Eaglehawk Neck, Tasmania, with his expert support and advice as a local diver.

Remarks

Several characters of *P. baroni*, sp. nov. are variable across specimens. This includes the number of oviger compound spines and teeth along the oviger claw margins as well as the number of major spines of the propodus heel (Fig. S1*D–F*). The latter may even differ between the left and right leg of one trunk segment. In most cases, there are three major heel spines, but propodi with two or four spines occur as well. The proboscis of some specimens shows an inconspicuous inflation about halfway along its length (Fig. 10*A′*) but the overall appearance does not deviate significantly from a bullet shape. In some individuals, the lateral processes are slightly shorter than in the holotype (Fig. 10*B′*) or the cephalon's mid-dorsal mound is a bit more acute in anterior view (Fig. 10*A″*). More conspicuously, the width of the gap between the closed chela fingers as well as the presence of a protrusion along the sclerotised cutting edge of the immoveable finger differs markedly between specimens (Fig. 10*D*). Further, the extent to which the anal tubercle overreaches lateral process of leg 4 varies between specimens (Fig. 10*B*, *B′*), but it is never shorter than the latter. The small teeth along the oviger claw margins may possess blunt rather than tapering tips (Fig. 10*F′*), presumably due to wear, as previously pointed out by Staples (2014*a*).

The morphologically closest congeners (other than the sympatric *P.* cf. *chevron*) are specimens from Victoria and New South Wales that have also been placed in the unresolved '*variabilis*' complex (Arango and Brenneis 2013). The form from New South Wales can be readily distinguished from *P. baroni*, sp. nov. and *P.* cf. *chevron* because of its very different colouration pattern, significantly larger size and morphological features such as the distinctly shorter anal tubercle. In contrast, differences to the '*variabilis*' form from Victoria are subtler and in need of reinvestigation with additional specimens for replication in genetic analyses.

Pallenella* cf. *chevron

(Fig. 1*D–F*, 11, S3*A′–D′*, *E–G*)

Pseudopallene ambigua (morphotype with red stripes). Stevenson, 2003: plate 2b.

Pseudopallene '*variabilis*' complex (morphotype with stripes). Arango & Brenneis, 2013: 428–30.

Material examined

QM S111244, 1 male (EN18 [DNA voucher]), 28 Oct. 2015, Cathedral in Waterfall Bay, Eaglehawk Neck, Tasmania, 15–20 m.

QM S111245, 2 males (EN19 [DNA voucher], 11b), 1 subadult (EN03 [DNA voucher]), 2 subadults (EN20, 11a_1), 1 free-living postlarval instar (11a_2), 22 & 28 Oct. 2015, Phoque Rock, Eaglehawk Neck, Tasmania, 13–17-m depth.

QM S111246, 1 male (GBTAS_02), 2 subadults (GBTAS_07&08), Oct. 2008, coastal waters near Eaglehawk Neck, 10–15-m depth.

QM S92224, 2 free-living postlarval instars (TAS17, TAS30a) – collected in 2007, DNA vouchers in Arango & Brenneis (2013).

Remarks

The Tasmanian *P.* cf. *chevron* agrees in many aspects with the description of the male *P. chevron* holotype from southern Australia. In addition to the distinctive stripes (Staples 2007), also the holotype's four major heel spines are in line with the most frequently observed number in the Tasmanian material, although even up to five heel spines were encountered in the latter (Fig. 11*F*), which contrasts with the more typical three spines of the similar *P. baroni*, sp. nov. A striking feature of *P.* cf. *chevron* is its somewhat variable proportion of chela length to height (Fig. 11*C–C‴*). Some specimens feature a palm that is almost as elongated as in *P. baroni*, sp. nov., whereas it is more compact in other individuals. In contrast,

Fig. 10. *Pallenella baroni*, sp. nov. 'Black tips' morphotype. (*A–A‴*) Anterior views of four specimens. Note different extent of the black marks on proboscis and chela fingers. (*A*) Male holotype (EN05). *A′*, Female (EN25). *A″*, Female (PSE3). Note marginally more acute mid-dorsal mound of cephalon. *A‴*, Freshly moulted male (Exp4_1). (*B*) Dorsal aspect of male holotype (EN05). *B′*, Dorsal aspect of female (PSE3b) partially covered by epibionts. (*C*) Lateral view of trunk (female, PSE3). (*D*) Right chelae in frontal and posterior view (top and bottom respectively). Left: male holotype (EN05). Middle: female (EN25). Right: Female (PSE3). Note varying extent of dark marks and variable width of gap between chela fingers. (*E*) Oviger of male holotype. (*F*, *F′*) Oviger article 10 (partial) and oviger claw (cLSM scans). (*F*) Male holotype (EN05). Note tapering but relatively round tips of teeth along the claw's margin. *F′*, Female (EN25). Note blunt tips of teeth along the claw's margin. (*G*) Leg of male holotype, with magnification of tarsus, propodus and main claw. Note three major unpaired heel spines (bracket) followed distally by a smaller pair (arrowhead) at the transition to the propodus sole. *G′*, Leg of female (5_1). Note proportionally shorter coxa 2 and swollen femur.

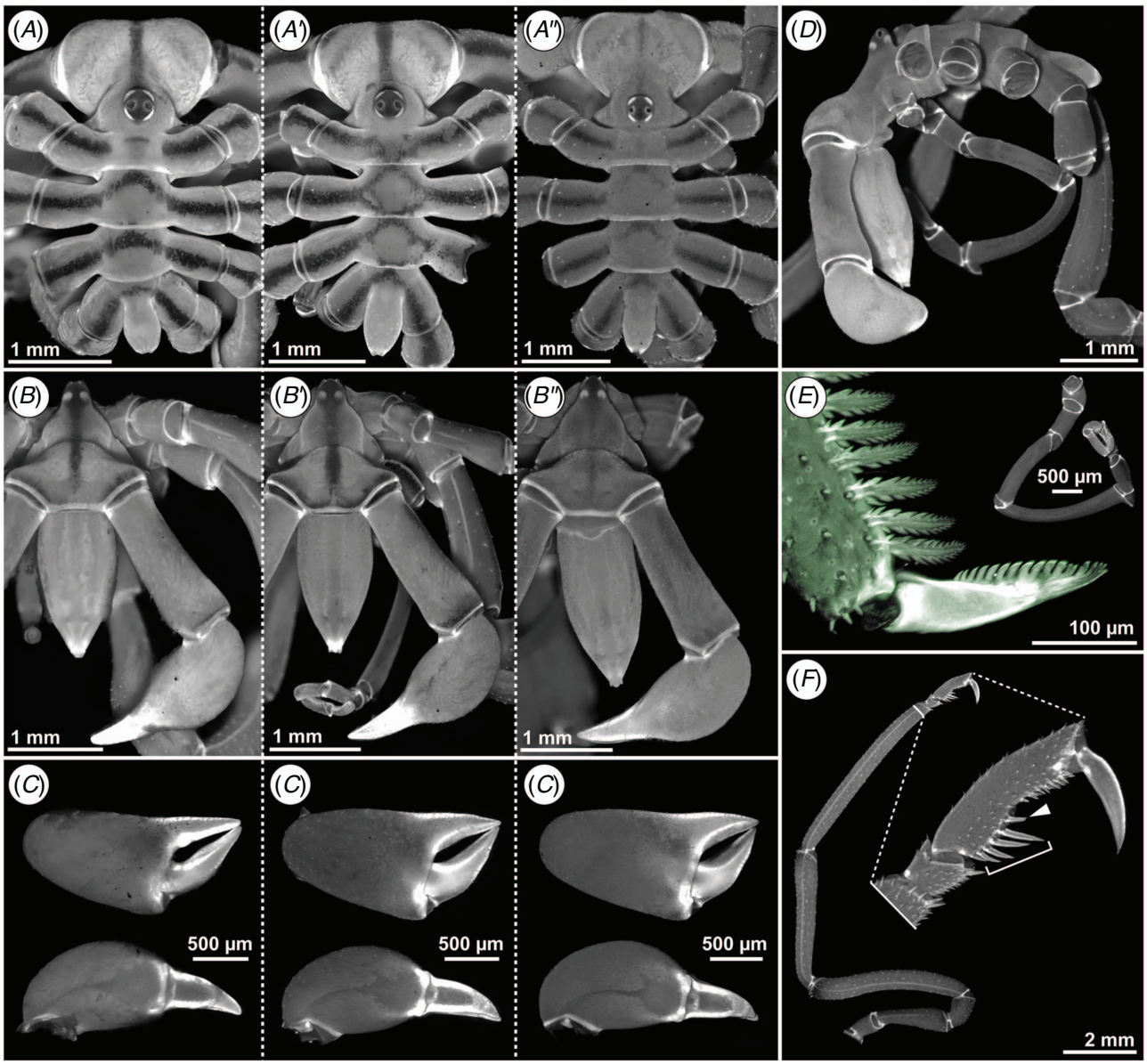

Fig. 11. *Pallenella* cf. *chevron*. 'Stripes' morphotype. (*A–A″*) Dorsal aspects of three specimens EN18, EN19 and 11b. Note slightly deviating pattern in EN19 (*A′*) and less intense stripes in formaldehyde-preserved 11b (*A″*). (*B–B″*) Anterior views of same specimens shown in *A–A″*. Note lack of black marks on proboscis and chela fingers. (*C–C″*) Right chelae in frontal and posterior view (top and bottom respectively), same specimens as in *A–A″*. Note shape differences in frontal view. (*D*) Lateral view of cephalon and trunk (11b). (*E*) Male oviger (top right corner) and detail of oviger article 10 and oviger claw (11b). Note relatively blunt and partially worn tips of teeth along the claw's margin. (*F*) Leg, with magnification of tarsus, propodus and main claw. Note five major heel spines (bracket) followed distally by a smaller pair (arrowhead) at the transition to the propodus sole.

the inflation of the palm appears to be marginally but consistently greater in *P.* cf. *chevron* than in *P. baroni*, sp. nov. (see above).

Invariable features of the pattern of red lines in the Tasmanian specimens studied are (1) a transverse line that looks like an upside-down 'V' (=chevron) on the dorsal side of trunk segments 2–4, continuing along the lateral process and coxae 1 and 2, (2) a red ocular tubercle with medial line extending anteriorly across the cephalon, (3) at least a hint of a transverse line along proboscis and scape insertions and (4) coxa 3 and femur with ventral longitudinal marks. In addition to this core pattern, red marks may occur in more distal regions, including (1) a longitudinal line laterally along the scape and a concentric ring around the distal scape margin plus marks on chela fingers (Fig. 1*E*), (2) also tibiae 1 and 2 ventrally with weak longitudinal lines, (3) the distal margins of coxae 2 and 3 as well as femur and tibia 1 with a narrow concentric ring (Fig. 1*D*, *F*), (4) tibia 2 and propodus occasionally with a broader but less distinct concentric band

(Fig. 1*D*′), (5) longitudinal lines on the outward facing sides of oviger articles, and (6) an additional 'V' posteriorly on cephalon and trunk segments 2 and 3 (Fig. 11*A*′).

Pallenella cf. ***ambigua***

(Fig. 2*B*, *C*, 12, 13*A*–*C*)

Material examined

QM S111247, 2 subadults (EN10&11 [both DNA vouchers]), 1 male (Exp8_1), 1 female (Exp8_2), 22 & 28 Oct. 2015, Phoque Rock, Eaglehawk Neck, Tasmania, 13–17-m depth. 1 male (EN07 [DNA voucher], 22 Oct. 2015, Phoque Rock, Eaglehawk Neck, Tasmania, 13–17-m depth.

QM S111248, 1 subadult (EN27 [DNA voucher]), 30 Oct. 2015, Cathedral in Waterfall Bay, Eaglehawk Neck, Tasmania, 18–21-m depth.

QM S111249, 1 female (Exp13_1), 2 males (Exp13_2&3), 1 subadult (Exp14_1), 6 Nov. 2015, Knobbies Wall, Eaglehawk Neck, Tasmania, 12–16-m depth.

Pallenella harrisi (Arango & Brenneis, 2013)

(Fig. 13*A*′–*C*′)

Pseudopallene harrisi Arango & Brenneis, 2013: 424–426, fig. 2*g*, 13*a*–*f*.
Meridionale harrisi Staples, 2014: 351–53, fig. 4*b, c*.

Material examined

QM S111250, 1 ovigerous male (NSW_03), 1 subadult (NSW_04), 29 Nov. 2009, Bass Point, New South Wales, 20-m depth.

QM S92225, 1 (subadult?) male (SHE010-1) – collected in 2009.

Pallenella gracilis (Arango & Brenneis, 2013)

(Fig. 14)

Pseudopallene gracilis Arango & Brenneis, 2013: 420–22, fig. 3*f*, 11*a*–*g*.
Meridionale gracilis Staples, 2014.

Material examined

QM S111251, 1 subadult male (TAS30 [DNA voucher]), 26 Jan. 2007, Waterfall Bay, Eaglehawk Neck, Tasmania, 18–21-m depth.

Remarks

Although the specimen studied is not a fully grown adult, its morphological assignment to *P. gracilis* is straightforward and confirmed by its *ITS* sequence, which matches the holotype (Fig. 4). In line with the subadult stage, the legs are still markedly shorter than in the adult holotype (9 *v*. 13.91 mm) and the number of ovigeral compound spines is lower as well (8 : 6 : 6 : 6 *v*. 13 : 9 : 6 : 7).

Notably, the subadult shows moderately inflated trunk segments and an upwardly directed anal tubercle (Fig. 14*D*), which is not mentioned in the description of the holotype (Arango and Brenneis 2013). As the orientation of the anal tubercle has never been observed to be subject to intraspecific variation in any congener, we are confident that a reinvestigation of the *P. gracilis* holotype will corroborate the finding of the current study. Further, in the specimen studied here, the cuticular jaws of the mouth form a short tube-like ridge with frayed distal margins (Fig. 14*A*, *B*), whereas the holotype has been described as bearing dark setae around the mouth opening (Arango and Brenneis 2013).

P. gracilis shares the acute preocular mid-dorsal mound, inflated segments, an upwardly inclined anal tubercle and a similar proboscis shape with *P. karenae*, sp. nov. and *P. inflata*. Yet, the division line of the mid-dorsal mound is restricted to the anterior base (Fig. 14*A*), the trunk segments are more evenly rounded (Fig. 14*D*) and segments 2 and 3 bear multiple dorsal setae in an unordered pattern (Fig. 14*E*, *F*). Moreover, its anal tubercle is inflated along its length (Fig. 14*E*), the moveable chela finger tapers towards a very delicate sharp tip that is as long as the immovable finger (Fig. 14*C*), and the oviger claw's margins are lined by a much higher number of very small teeth (Fig. 14*G*). Finally, the cuticular sockets of the setae on the leg podomeres are bulbous and protrude notably (Fig. 14*H*), conveying the impression that *P. gracilis* is covered in tiny spines, whereas the leg setae of *P. karenae*, sp. nov. and *P. inflata* are less conspicuous (Fig. 8*G*, 9*H*). Owing to this combination of characters, *P. gracilis* can be readily separated from *P. karenae*, sp. nov. and *P. inflata*.

Pallenella tasmania (Arango & Brenneis, 2013)

(Fig. 15)

Pseudopallene tasmania Arango & Brenneis, 2013: 417, fig. 7*a*–*h*.
Meridionale tasmania Staples, 2014: 353.

Material examined

QM S111252, 1 subadult female (EN28 [DNA voucher]), 30 Oct. 2015, Cathedral in Waterfall Bay, Eaglehawk Neck, Tasmania, 18–21-m depth.

QM S92217, 2 subadults (TAS21a, TAS35a) – collected in 2007, DNA vouchers in Arango & Brenneis (2013).

Remarks

Both molecular markers unambiguously assign the new 2015 individual to *P. tasmania* and also, at the morphological level, it shows the diagnostic features of *P. tasmania* (very high ovigeral spine count, almost straight propodus with inconspicuous heel, inner margin of main claw almost straight). In line with Staples' observations on the holotype and two paratypes (Staples 2014*a*), the margins of the ovigeral claw are very delicately denticulated (Fig. 15*B*, *B*′). The minute teeth of these denticulations are in part worn down (Fig. 15*B*′), which may give the impression of a crenulation, as originally reported for the holotype (Arango and Brenneis 2013). In further agreement with Staples (2014*a*), the new specimen and the two other subadults studied have a proboscis with a slight constriction at mid-length and a marginally upwardly inclined anal tubercle. Notably, the new specimen had a yellow body colouration when live (Fig. 15*A*), differing from the semitransparent appearance with reddish midgut diverticula observed in live material from 2009 (Arango and Brenneis 2013). This indicates a certain variation in the general body colouration of *P. tasmania*, potentially depending on the nutritional state of individuals at the time of collection.

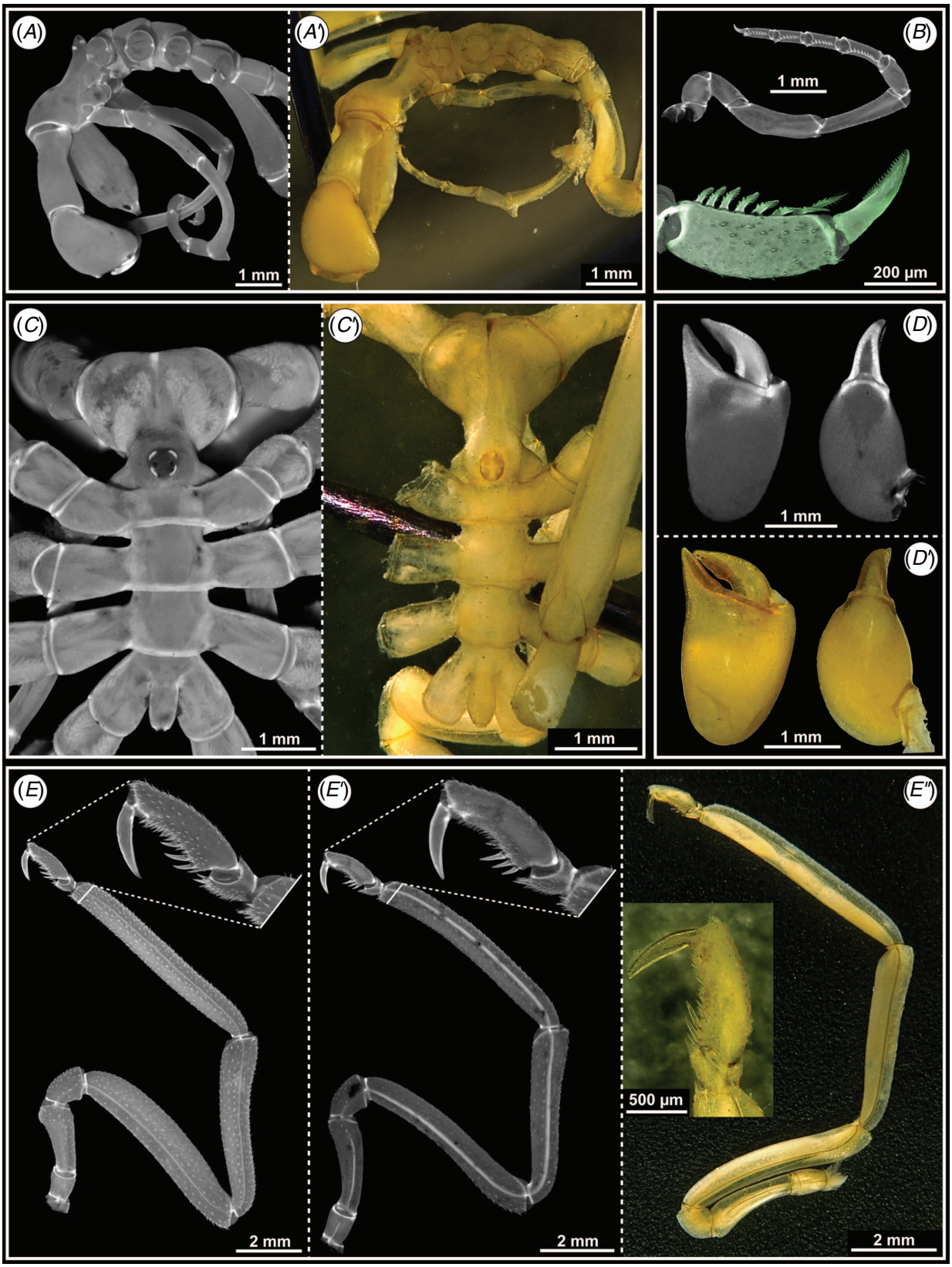

Fig. 12. Comparison of Tasmanian *Pallenella* cf. *ambigua* with holotype of *P. ambigua* (Stock, 1956). Tasmanian *P.* cf. *ambigua* shown in grayscale epifluorescence images, holotype (Zoologisches Museum Hamburg, voucher number K17680) shown in brightfield stereomicroscopic images. (*A*, *A*′) Lateral view of cephalon and trunk. (*B*) Oviger of female (top) and detail of oviger article 10 and oviger claw (bottom, cLSM scan). (*C*, *C*′) Dorsal aspect. (*D*, *D*′) Right chela in frontal and posterior view (left and right respectively). (*E*–*E*″) Leg with magnification of tarsus, propodus and main claw. Female and male of *P.* cf. *ambigua* shown (*E* and *E*′ respectively).

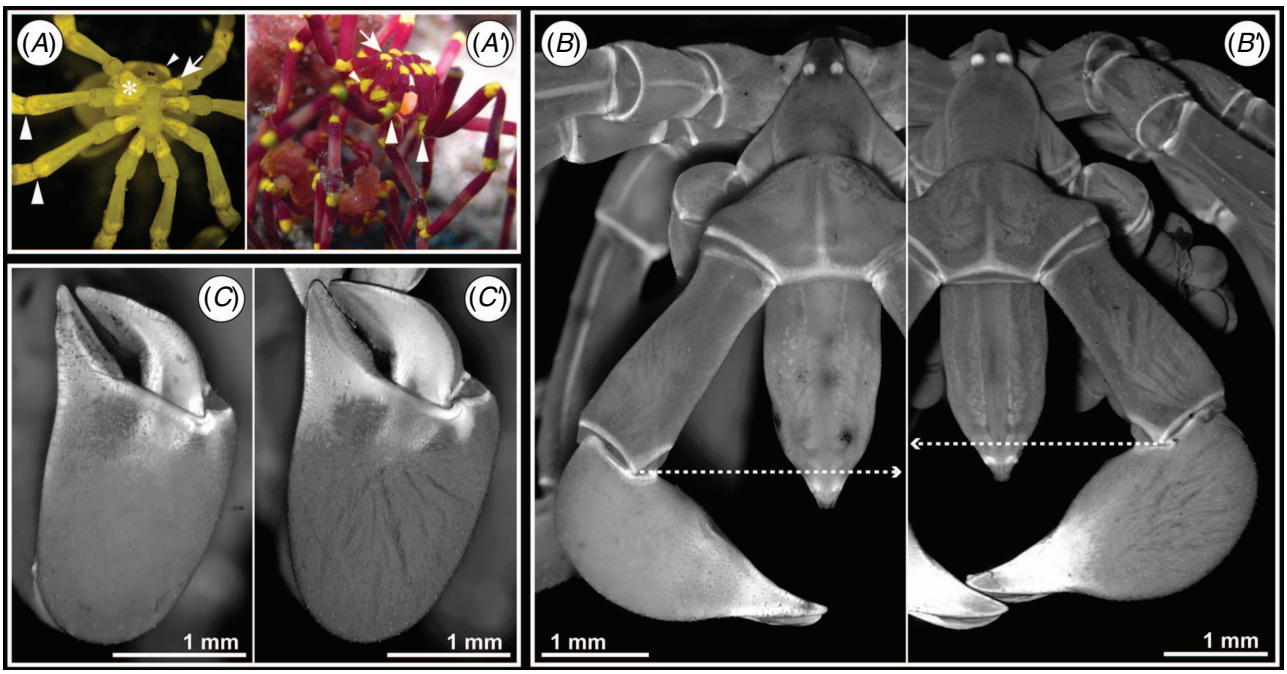

Fig. 13. Comparison of Tasmanian *Pallenella* cf. *ambigua* with *P. harrisi* (Arango & Brenneis, 2013). *P.* cf. *ambigua* always on the left, *P. harrisi* on the right. (*A*, *A*′) Live specimens. Note corresponding yellow marks on lateral processes (arrow), cephalon (small arrowhead) and coxae 2 and 3 (large arrowheads). Asterisks mark an epibiont. (*B*, *B*′) Frontal view. Note proportionately shorter scape (stippled arrows) and more bulbous chela in *P. harrisi*. (*C*, *C*′) Chela, frontal view. Note more robust chela fingers in *P. harrisi*.

Pallenella pachycheira (Haswell, 1884)

Pallene pachycheira Haswell, 1884: 1030–1031, pl. 57, fig. 6–9.
Parapallene pachycheira Loman, 1908: 47–48.
Pseudopallene pachycheira Flynn, 1919: 77–79, fig. 9–11; Stock, 1956: 42; Staples, 1997: 1053, fig. 21.3*d*; 2008: 131; Arango & Brenneis, 2013: 420, fig. 2*f*, 10*a–d*.
Meridionale pachycheira Staples, 2014.

Material examined

QM S111253, 1 young female (EN21 [DNA voucher]), 30 Oct. 2015, Cathedral in Waterfall Bay, Eaglehawk Neck, Tasmania, 18–21-m depth.

QM S111254, 1 female (EN35 [DNA voucher]), 6 Nov. 2015, Boulder Point, Eaglehawk Neck, Tasmania, 10-m depth. 1 male (EN01 [DNA voucher]), 21 Oct. 2015, Waterfall Bay, Eaglehawk Neck, Tasmania, 10-m depth.

QM S92220, 1 female (PSE8), 1 subadult (PSE11a) – collected in 2009, DNA vouchers in Arango & Brenneis (2013).

Remarks

Morphological assignment of the new specimens to *P. pachycheira* is confirmed by the similarity in the *ITS* fragment compared to specimens from 2007 and 2009 (Arango and Brenneis 2013). The first available *COI* sequences add further support to the species status of *P. pachycheira* (*p*-distances >11.3% to congeners). Notably, the tips of the proboscis and chela fingers of one specimen (EN21) show a dark crust similar to those of *P. baroni*, sp. nov. and some specimens of *P.* cf. *chevron* and *P. inflata*.

Pallenella reflexa (Stock, 1968)

Spasmopallene reflexa Stock, 1968: 40–42, fig. 1*A–H*.
Pseudopallene reflexa Staples, 2005: 164–166, fig. 4*A–G*; Staples 2007: 99; Staples 2008: 129, fig. 2*C, D*; Arango & Brenneis 2013: 417–18, fig. 8*A–D*.
Meridionale reflexa Staples, 2014.

Material examined

QM S111255, 1 male (EN29 [DNA voucher]), 30 Oct. 2015, Cathedral in Waterfall Bay, Eaglehawk Neck, Tasmania, 18–21-m depth.

QM S111256, 1 female (EN33 [DNA voucher]), 6 Nov. 2015, Knobbies Wall, Eaglehawk Neck, Tasmania, 12–16-m depth.

QM S92218, 1 female (PSE5a), 2 males (PSE5, 5b), 1 subadult (PSE11) – collected in 2009, DNA vouchers in Arango & Brenneis (2013).

QM S111257, 1 female (GBTAS_09), 1 male (GBTAS_10), Oct. 2008, coastal waters near Eaglehawk Neck, Tasmania, 10–18-m depth.

Remarks

Morphology and *ITS* sequences of the new specimens are in good agreement with material previously studied (Arango and Brenneis 2013). The new 595-bp *COI* fragment further validates the species status of *P. reflexa* (*p*-distance >13.5% to other congeners).

Ethics

All specimens were collected under permits of the Tasmanian Department of Primary Industries, Parks, Water and Environment (permit numbers 6039, 7111, 9255, 15111).

Data accessibility

All sequence data are deposited in GenBank. The study has been registered at ZooBank: urn:lsid:zoobank.org:pub:9CE2B869-7F6A-4690-912F-71F072327484.

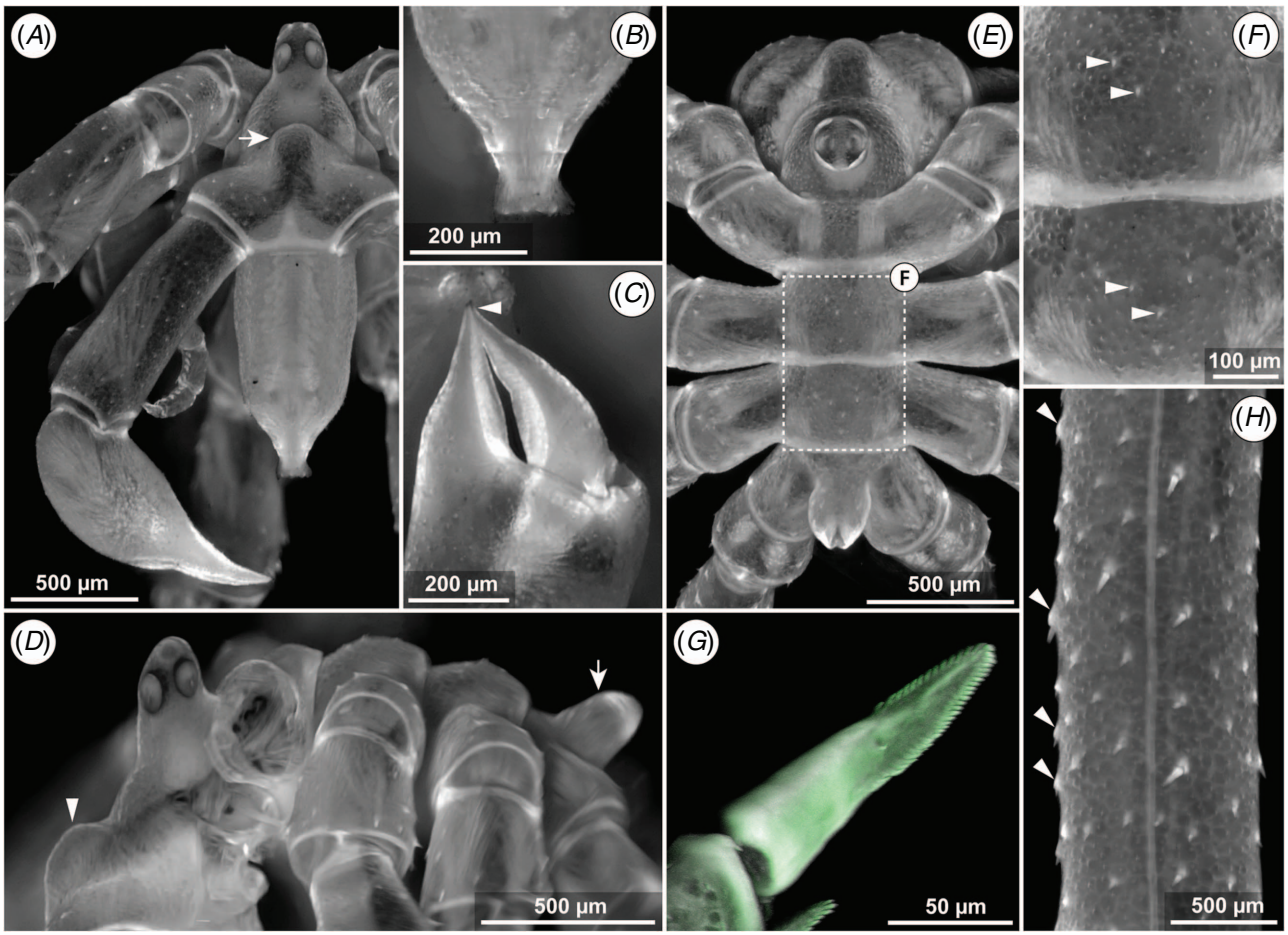

Fig. 14. *Pallenella gracilis* (Arango & Brenneis, 2013). Subadult from Tasmania (TAS30). Note that dark midgut diverticula are visible through the semitransparent cuticle. (*A*) Anterior view. Note acute preocular mound without longitudinal division line (arrow). (*B*) Proboscis tip. The extended jaws form a short tube that protrudes around the mouth. (*C*) Chela fingers. Note tapering of moveable finger to sharply pointed tip (arrowhead), as long as the immoveable counterpart. (*D*) Lateral view of trunk. Note mid-dorsal mound on cephalon (arrowhead), evenly rounded trunk segments and upwardly inclined anal tubercle (arrow). (*E*) Dorsal aspect. (*F*) Detail of trunk segments 2 and 3, dorsal view (area indicated by inset in *E*). Note irregular array of small setae (exemplarily highlighted by arrowheads). (*G*) Detail of oviger claw (cLSM scan). Note very fine teeth along both margins of the claw. (*H*) Detail of tibia 2. Note bulbous sockets of setae (arrowheads) and longitudinal cuticular ridge.

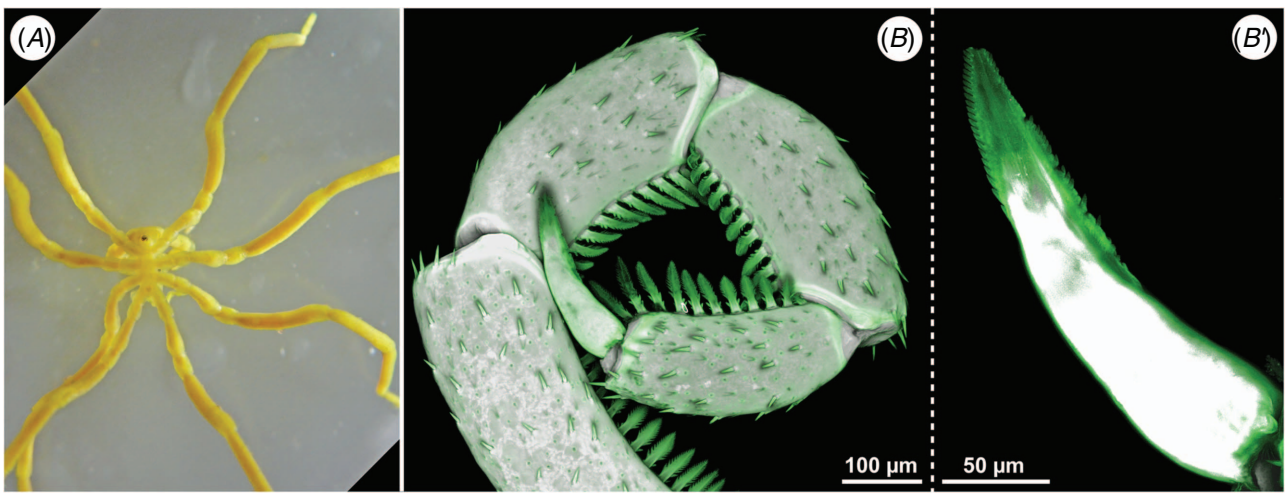

Fig. 15. *Pallenella tasmania* (Arango & Brenneis, 2013). Subadult female (EN28). (*A*) Live specimen. Note yellow colouration. (*B*, *B*′) Details of oviger articles 7–10 and oviger claw (cLSM scans). Note high number of oviger compound spines (*B*) and minute, partially worn teeth along the claw's margins (*B*′).

Author contributions

G. Brenneis and C. P. Arango devised the study and collected the specimens. G. Brenneis performed morphological analyses and documentation. G. Brenneis, C. P. Arango and P. P. Sharma performed molecular work. M. Schwentner performed analyses of molecular data. G. Brenneis drafted the manuscript. All authors discussed and edited further drafts and approved the final version.

Conflicts of interest

P. P. Sharma is an Associate Editor for *Invertebrate Systematics*. Despite this relationship, he did not at any stage have Associate Editor-level access to this manuscript while in peer review, as is the standard practice when handling manuscripts submitted by an editor to this journal. *Invertebrate Systematics* encourages its editors to publish in the journal and they are kept totally separate from the decision-making process for their manuscripts. The authors have no further conflicts of interest to declare.

Declaration of Funding

G. Brenneis is funded by the Deutsche Forschungsgemeinschaft (grant number BR5039/3-1; specimen collection in 2015 under grant number BR5039/1-1). Molecular work performed by G. Brenneis was funded by a National Science Foundation grant to Barbara S. Beltz (NSF-IOS-1656103). Some of the material for this study was collected and analysed with financial support of the Australian Biological Resources Studies (ABRS grant number 204-61) to C. P. Arango.

Acknowledgements

We thank Karen Gowlett-Holmes, Mick Baron and Ben and Pauline Nuttens of the Eaglehawk Dive Centre for their extensive help during all collection trips to Tasmania. G. Brenneis is indebted to Barbara Beltz for contributing funds to the 2015 collection trip and hosting him in her laboratory at Wellesley College, MA, during the molecular work for the study. David Staples is thanked for his advice regarding new Tasmanian morphotypes and for sharing an unpublished image of *P. karenae* sp. nov. from Victoria. Markus Koch and Hieronymus Dastych from the Zoological Museum Hamburg, Germany, are acknowledged for their assistance with the re-investigation of the *P. ambigua* holotype. Andrea Crowther from the South Australian Museum, Adelaide, is thanked for providing photographs of the marks on the *P. chevron* holotype. Emily V. W. Setton assisted with cataloguing and extraction of *Pallenella* specimens at UW-Madison. The constructive comments of three anonymous reviewers helped to improve the manuscript.

References

Arango, C. P. (2009). New species and new records of sea spiders (Arthropoda: Pycnogonida) from deep waters in Western Australia. *Zootaxa* **1977**, 1–20. doi:10.11646/zootaxa.1977.1.1

Arango, C. P., and Brenneis, G. (2013). New species of Australian *Pseudopallene* (Pycnogonida: Callipallenidae) based on live colouration, morphology and DNA. *Zootaxa* **3616**, 401–436. doi:10.11646/zootaxa.3616.5.1

Arango, C. P., and Linse, K. (2015). New *Sericosura* (Pycnogonida: Ammotheidae) from deep-sea hydrothermal vents in the Southern Ocean. *Zootaxa* **3995**, 37–50. doi:10.11646/zootaxa.3995.1.5

Arango, C. P., Soler-Membrives, A., and Miller, K. J. (2011). Genetic differentiation in the circum-Antarctic sea spider *Nymphon australe* (Pycnogonida; Nymphonidae). *Deep-sea Research – II. Topical Studies in Oceanography* **58**, 212–219. doi:10.1016/j.dsr2.2010.05.019

Arnaud, F., and Bamber, R. N. (1987). The biology of Pycnogonida. *Advances in Marine Biology* **24**, 1–96.

Ballesteros, J. A., Santibánez Lopéz, C. E., Kovác, L., Gavish-Regev, E., and Sharma, P. P. (2019). Ordered phylogenomic subsampling enables diagnosis of systematic errors in the placement of the enigmatic arachnid order Palpigradi. *Proceedings of the Royal Society of London – B. Biological Sciences* **286**, 20192426. doi:10.1098/rspb.2019.2426

Ballesteros, J. A., Setton, E. V. W., Santibánez López, C. E., Arango, C. P., Brenneis, G., Brix, S., Cano-Sánchez, E., Dandouch, M., Dilly, G. F., Eleaume, M. P., Gainett, G., Gallut, C., McAtee, S., McIntyre, L., Moran, A. L., Moran, R., López-González, P. J., Scholtz, G., Williamson, C., Woods, H. A., Wheeler, W. C., and Sharma, P. P. (2020). Phylogenomic resolution of sea spider diversification through integration of multiple data classes. *bioRxiv* [Preprint posted on 4 February 2020]. doi:10.1101/2020.01.31.929612

Bamber, R. N. (2010). 'Sea-Spiders (Pycnogonida) of the North-east Atlantic', 2nd edn. (Field Studies Council Publications: Shrewsbury, UK.)

Bamber, R. N., El Nagar, A., and Arango, C. P. (2020). Pycnobase: World Pycnogonida Database. In 'World Register of Marine Species'. (Integrated Marine Information System.) Available at http://www.marinespecies.org/imis.php?dasid=970&doiid=360 [Verified 13 August 2020].

Blackman, A., and Walls, J. (1995). Bryozoan secondary metabolites and their chemical ecology. In 'Studies in Natural Product Chemistry. Vol 17: Structure and Chemistry (Part D)'. (Ed. Atta-ur-Rahman.) pp. 77–112. (Elsevier.)

Brenneis, G., and Arango, C. P. (2019). First description of epimorphic development in Antarctic Pallenopsidae (Arthropoda, Pycnogonida) with insights into the evolution of the four-articled sea spider cheliphore. *Zoological Letters* **5**, 4. doi:10.1186/s40851-018-0118-7

Brenneis, G., and Scholtz, G. (2014). The 'ventral organs' of Pycnogonida (Arthropoda) are neurogenic niches of late embryonic and post-embryonic nervous system development. *PLoS One* **9**, e95435. doi:10.1371/journal.pone.0095435

Brenneis, G., Arango, C. P., and Scholtz, G. (2011*a*). Morphogenesis of *Pseudopallene* sp. (Pycnogonida, Callipallenidae). I: Embryonic development. *Development Genes and Evolution* **221**, 309–328. doi:10.1007/s00427-011-0382-4

Brenneis, G., Arango, C. P., and Scholtz, G. (2011*b*). Morphogenesis of *Pseudopallene* sp. (Pycnogonida, Callipallenidae). II: Postembryonic development. *Development Genes and Evolution* **221**, 329–350. doi:10.1007/s00427-011-0381-5

Brenneis, G., Stollewerk, A., and Scholtz, G. (2013). Embryonic neurogenesis in *Pseudopallene* sp. (Arthropoda, Pycnogonida) includes two subsequent phases with similarities to different arthropod groups. *EvoDevo* **4**, 32. doi:10.1186/2041-9139-4-32

Brenneis, G., Bogomolova, E. V., Arango, C. P., and Krapp, F. (2017). From egg to 'no-body': an overview and revision of developmental pathways in the ancient arthropod lineage Pycnogonida *Frontiers in Zoology* **14**, 6. doi:10.1186/s12983-017-0192-2

Brenneis, G., Scholtz, G., and Beltz, B. (2018). Comparison of ventral organ development across Pycnogonida (Arthropoda, Chelicerata) provides evidence for a plesiomorphic mode of late neurogenesis in sea spiders and myriapods. *BMC Evolutionary Biology* **18**, 47. doi:10.1186/s12862-018-1150-0

Brusca, R. C., and Brusca, G. J. (2003). 'Invertebrates', 2nd edn. (Sinauer Associates, Inc.: Sunderland, MA, USA.)

Cano-Sánchez, E., and López-González, P. J. (2019). Two new species and new findings in the genus *Pallenopsis* (Pycnogonida:

Pallenopsidae) with an updated identification key to Antarctic and sub-Antarctic species. *Zootaxa* **4585**, 517–530. doi:10.11646/zootaxa.4585.3.7

Clark, W. C. (1963). Australian Pycnogonida. *Records of the Australian Museum* **26**, 1–82. doi:10.3853/j.0067-1975.26.1963.669

Collins, E., Galaska, M., Halanych, K. M., and Mahon, A. R. (2018). Population genomics of *Nymphon australe* Hodgson, 1902 (Pycnogonida, Nymphonidae) in the western Antarctic. *The Biological Bulletin* **234**, 180–191. doi:10.1086/698691

Dietz, L., Krapp, F., Hendrickx, M. E., Arango, C. P., Krabbe, K., Spaak, J. M., and Leese, F. (2013). Evidence from morphological and genetic data confirms that *Colossendeis tenera* Hilton, 1943 (Arthropoda: Pycnogonida), does not belong to the *Colossendeis megalonyx* Hoek, 1881 complex. *Organisms, Diversity & Evolution* **13**, 151–162. doi:10.1007/s13127-012-0120-4

Dietz, L., Arango, C. P., Dömel, J. S., Halanych, K. M., Harder, A. M., Held, C., Mahon, A. R., Mayer, C., Melzer, R. R., Rouse, G. W., Weis, A., Wilson, N. G., and Leese, F. (2015*a*). Regional differentiation and extensive hybridization between mitochondrial clades of the Southern Ocean giant sea spider *Colossendeis megalonyx*. *Royal Society Open Science* **2**, 140424. doi:10.1098/rsos.140424

Dietz, L., Pieper, S., Seefeldt, M. A., and Leese, F. (2015*b*). Morphological and genetic data clarify the taxonomic status of *Colossendeis robusta* and *C. glacialis* (Pycnogonida) and reveal overlooked diversity. *Arthropod Systematics & Phylogeny* **73**, 107–128.

Dömel, J. S., Convey, P., and Leese, F. (2015). Genetic data support independent glacial refugia and open ocean barriers to dispersal for the Southern Ocean sea spider *Austropallene cornigera* (Möbius, 1902). *Journal of Crustacean Biology* **35**, 480–490. doi:10.1163/1937240X-00002351

Dömel, J. S., Melzer, R. R., Harder, A. M., Mahon, A. R., and Leese, F. (2017). Nuclear and mitochondrial gene data support recent radiation within the sea spider species complex *Pallenopsis patagonica*. *Frontiers in Ecology and Evolution* **4**, 139. doi:10.3389/fevo.2016.00139

Dömel, J. S., Macher, T.-H., Dietz, L., Duncan, S., Mayer, C., Rozenberg, A., Wolcott, K., Leese, F., and Melzer, R. R. (2019). Combining morphological and genomic evidence to resolve species diversity and study speciation processes of the *Pallenopsis patagonica* (Pycnogonida) species complex. *Frontiers in Zoology* **16**, 36. doi:10.1186/s12983-019-0316-y

Dömel, J. S., Dietz, L., Macher, T.-H., Rozenberg, A., Mayer, C., Spaak, J. M., Melzer, R. R., and Leese, F. (2020). Analyzing drivers of speciation in the Southern Ocean using the sea spider species complex *Colossendeis megalonyx* as a test case. *Polar Biology* **43**, 319–342. doi:10.1007/s00300-020-02636-z

Dunlop, J. A., and Arango, C. P. (2005). Pycnogonid affinities: a review. *Journal of Zoological Systematics and Evolutionary Research* **43**, 8–21. doi:10.1111/j.1439-0469.2004.00284.x

Dunlop, J. A., and Lamsdell, J. C. (2017). Segmentation and tagmosis in Chelicerata. *Arthropod Structure & Development* **46**, 395–418. doi:10.1016/j.asd.2016.05.002

Flynn, T. T. (1919). A re-examination of Professor Haswell's types of Australian Pycnogonida. *Papers and Proceedings of the Royal Society of Tasmania* **1919**, 70–92. doi:10.5962/bhl.part.21284

Folmer, O., Black, M., Hoeh, W., Lutz, R., and Vrijenhoek, R. (1994). DNA primers for amplification of mitochondrial cytochrome *c* oxidase subunit I from diverse metazoan invertebrates. *Molecular Marine Biology and Biotechnology* **3**, 294–299.

Griffiths, H. J., Arango, C. P., Munilla, T., and McInnes, S. J. (2011). Biodiversity and biogeography of Southern Ocean pycnogonids. *Ecography* **34**, 616–627. doi:10.1111/j.1600-0587.2010.06612.x

Harder, A. M., Halanych, K. M., and Mahon, A. R. (2016). Diversity and distribution within the sea spider genus *Pallenopsis* (Chelicerata: Pycnogonida) in the western Antarctic as revealed by mitochondrial DNA. *Polar Biology* **39**, 677–688. doi:10.1007/s00300-015-1823-8

Haswell, W. A. (1884). On the Pycnogonida of the Australian coast, with descriptions of new species. *Proceedings of the Linnean Society of New South Wales* **9**, 1021–1034.

Hebert, P., Cywinska, A., Ball, S., and deWaard, J. (2003). Biological identifications through DNA barcodes. *Proceedings of the Royal Society of London – B. Biological Sciences* **270**, 313–321. doi:10.1098/rspb.2002.2218

Hoek, P. P. C. (1881). Report on the Pycnogonida, dredged by H.M. S. Challenger during the years 1873–76. *Challenger Reports, Zoology* **3**(10), 1–167.

Katoh, K., and Standley, D. (2013). MAFFT multiple sequence alignment software version 7: improvements in performance and usability. *Molecular Biology and Evolution* **30**, 772–780. doi:10.1093/molbev/mst010

Kekkonen, M., and Hebert, P. (2014). DNA barcode-based delineation of putative species: efficient start for taxonomic workflows. *Molecular Ecology Resources* **14**, 706–715. doi:10.1111/1755-0998.12233

Kim, I.-H., and Hong, J.-S. (1987). *Bradypallene espina*, new genus and new species, a pycnogonid from the East Sea of Korea (Pycnogonida). *Tongmul Hakhoe Chi* **30**, 272–276.

Krabbe, K., Leese, F., Mayer, C., Tollrian, R., and Held, C. (2010). Cryptic mitochondrial lineages in the widespread pycnogonid *Colossendeis megalonyx* Hoek, 1881 from Antarctic and sub-Antarctic waters. *Polar Biology* **33**, 281–292. doi:10.1007/s00300-009-0703-5

Kumar, S., Stecher, G., Li, M., Knyaz, C., and Tamura, K. (2018). MEGA X: Molecular Evolutionary Genetics Analysis across computing platforms. *Molecular Biology and Evolution* **35**, 1547–1549. doi:10.1093/molbev/msy096

Legg, D. A., Sutton, M. D., and Edgecombe, G. D. (2013). Arthropod fossil data increase congruence of morphological and molecular phylogenies. *Nature Communications* **4**, 2485. doi:10.1038/ncomms3485

Lotz, G., and Bückmann, D. (1968). Die Häutung und die Exuvie von *Pycnogonum litorale* (Ström) (Pantopoda). *Zoologische Jahrbücher, Abteilung für Anatomie und Ontogonie der Tiere* **85**, 529–536.

Lozano-Fernandez, J., Tanner, A. R., Giacomelli, M., Carton, R., Vinther, J., Edgecombe, G. D., and Pisani, D. (2019). Increasing species sampling in chelicerate genomic-scale datasets provides support for monophyly of Acari and Arachnida. *Nature Communications* **10**, 2295. doi:10.1038/s41467-019-10244-7

Lucena, R. A., de Araújo, J. P., and Christoffersen, M. L. (2019). Pycnogonida (Arthropoda) from coral reef environments along the southwest Atlantic: new records and new species. *Marine Biology Research* **15**, 476–499. doi:10.1080/17451000.2019.1674876

Mahon, A. R., Arango, C. P., and Halanych, K. M. (2008). Genetic diversity of *Nymphon* (Arthropoda: Pycnogonida: Nymphonidae) along the Antarctic Peninsula with a focus on *Nymphon australe* Hodgson 1902. *Marine Biology* **155**, 315–323. doi:10.1007/s00227-008-1029-5

Meyer, K. E., and Bückmann, D. (1963). Die Häutungen des Pantopoden *Pycnogonum litorale* (Ström.). In 'Verhandlungen der Deutschen Zoologischen Gesellschaft in Wien 1962', Zoologischer Anzeiger Supplement 26, pp. 604–609. (Akad. Verl.gesell. Geest & Portig: Leipzig, East Germany.)

Morgan, E. (1977). The swimming of *Nymphon gracile* (Pycnogonida): the energetics of swimming at constant depth. *The Journal of Experimental Biology* **71**, 205–211.

Müller, H.-G., and Krapp, F. (2009). The pycnogonid fauna (Pycnogonida, Arthropoda) of the Tayrona National Park and adjoining areas on the Caribbean coast of Colombia. *Zootaxa* **2319**(1), 1–138. doi:10.11646/zootaxa.2319.1.1

Munilla, T., and Soler-Membrives, A. (2009). Check-list of the pycnogonids from Antarctic and sub-Antarctic waters: zoogeographic

implications. *Antarctic Science* **21**, 99–111. doi:10.1017/S0954102008001510X

Pagès, F., Corbera, J., and Lindsay, D. (2007). Piggybacking pycnogonids and parasitic narcomedusae on *Pandea rubra* (Anthomedusae, Pandeidae). *Plankton & Benthos Research* **2**, 83–90. doi:10.3800/pbr.2.83

Puillandre, N., Lambert, A., Brouillet, S., and Achaz, G. (2012). ABGD, Automatic Barcode Gap Discovery for primary species delimitation. *Molecular Ecology* **21**, 1864–1877. doi:10.1111/j.1365-294X.2011.05239.x

Ronquist, F., Teslenko, M., van der Mark, P., Ayres, D., Darling, A., Höhna, S., Larget, B., Liu, L., Suchard, M., and Huelsenbeck, J. (2012). Efficient Bayesian phylogenetic inference and model selection across a large model space. *Systematic Biology* **61**, 539–542. doi:10.1093/sysbio/sys029

Sabroux, R., Hassanin, A., and Corbari, L. (2019). Four times more species of sea spiders (Arthropoda: Pycnogonida) in Martinique Island (Lesser Antilles). *Marine Biodiversity* **49**, 1519–1535. doi:10.1007/s12526-019-00957-9

Sars, G. O. (1891). 'The Norwegian North-Atlantic Expedition 1876–1878. Zoology. Pycnogonidea.' (Christiania, Grøndahl & Søns.)

Schimkewitsch, W. (1909). Nochmals über die Periodicität in dem System der Pantopoden. *Zoologischer Anzeiger* **34**, 1–13.

Schwentner, M., Timms, B. V., and Richter, S. (2011). An integrative approach to species delineation incorporating different species concepts: a case study of *Limnadopsis* (Branchiopoda: Spinicaudata). *Biological Journal of the Linnean Society. Linnean Society of London* **104**, 575–599. doi:10.1111/j.1095-8312.2011.01746.x

Sherwood, J., Walls, J. T., and Ritz, D. A. (1998). Amathamide alkaloids in the pycnogonid, *Stylopallene longicauda*, epizoic on the chemically defended bryozoan, *Amathia wilsoni*. *Papers and Proceedings of the Royal Society of Tasmania* **132**, 65–70. doi:10.26749/rstpp.132.65

Soler-Membrives, A., Linse, K., Miller, K. J., and Arango, C. P. (2017). Genetic signature of Last Glacial Maximum regional refugia in a circum-Antarctic sea spider. *Royal Society Open Science* **4**, 170615. doi:10.1098/rsos.170615

Stamatakis, A. (2014). RAxML version 8: a tool for phylogenetic anaylses and post-analysis of large phylogenies. *Bioinformatics* **30**, 1312–1313. doi:10.1093/bioinformatics/btu033

Staples, D. (1997). Sea spiders or pycnogonids (Phylum Arthropoda). In 'Marine Invertebrates of Southern Australia. Part III'. (Eds S. A. Shepherd, and M. Davies.) pp. 1040–1072. (Government Printer: Adelaide, SA, Australia.)

Staples, D. (2005). Pycnogonida from the Althorpe Islands, South Australia. *Transactions of the Royal Society of South Australia* **129**, 158–169.

Staples, D. (2007). Pycnogonids (Arthropoda: Pycnogonida) from the Great Australian Bight, southern Australia, with description of two new species. *Memoirs of the Museum of Victoria* **64**, 95–101. doi:10.24199/j.mmv.2007.64.9

Staples, D. (2008). Investigator Group expedition 2006: Pycnogonida. *Transactions of the Royal Society of South Australia* **132**, 125–133. doi:10.1080/03721426.2008.10887098

Staples, D. (2014*a*). A revision of the callipallenid genus *Pseudopallene* Wilson, 1878 (Pycnogonida, Callipallenidae). *Zootaxa* **3765**, 339–359. doi:10.11646/zootaxa.3765.4.3

Staples, D. (2014*b*). A reassessment of the pycnogonid genus *Stylopallene* (Arthropoda, Callipallenidae) with description of a new genus. *Memoirs of the Museum of Victoria* **72**, 121–129. doi:10.24199/j.mmv.2014.72.07

Staples, D. A. (2015). A reassessment of the pycnogonid genus *Cheilopallene* (Arthropoda, Callipallenidae) with description of a new species from Papua New Guinea. *Zootaxa* **3995**, 51–57. doi:10.11646/zootaxa.3995.1.6

Staples, D. (2019). Pycnogonids (Arthropoda, Pycnogonida) from the Southwest Indian Ridge. *Zootaxa* **4567**, 401–449. doi:10.11646/zootaxa.4567.3.1

Staples, D. A. (2020). *Labrumoides vibrissa* (Arthropoda: Pycnogonida), new callipallenid genus and new species from north Western Australia. *Zootaxa* **4751**, 575–581.

Stevenson, D. (2003). Resolving a taxonomic ambiguity: variation in the pycnogonid *Pseudopallene ambigua* (Stock 1956). B.Sc.(Honours) Thesis, University of Tasmania.

Stock, J. H. (1956). Pantopoden aus dem Zoologischen Museum Hamburg. *Mitteilungen aus dem Hamburgischen Zoologischen Museum und Instituts* **54**, 33–48.

Stock, J. H. (1973). Pycnogonida from south-eastern Australia. *Beaufortia* **266**, 99–127.

Weis, A., Meyer, R., Dietz, L., Dömel, J. S., Leese, F., and Melzer, R. R. (2014). *Pallenopsis patagonica* (Hoek, 1881) – a species complex revealed by morphology and DNA barcoding, with description of a new species of *Pallenopsis* Wilson, 1881. *Zoological Journal of the Linnean Society* **170**, 110–131. doi:10.1111/zoj.12097

Wörheide, G. (1998). The reef cave dwelling ultraconservative corralline demosponge *Astrosclera willeyana* Lister 1900 from the Indo-Pacific. *Facies* **38**, 1–88. doi:10.1007/BF02537358

Wu, M., Chatterji, S., and Eisen, J. (2012). Accounting for alignment uncertainty in phylogenomics. *PLoS One* **7**, e30288. doi:10.1371/journal.pone.0030288

Handling editor: Gonzalo Giribet